ZIBELINE INTERNATIONAL™ PUBLISHING

ISSN: 2616-4302 (Online)
CODEN: AMMCFL

Acta Mechanica Malaysia (AMM)

DOI: http://doi.org/10.26480/amm.01.2024.60.77

RESEARCH ARTICLE

EVALUATION AND THERMAL-ANALYSIS OF A SOLAR-ASSISTED DRYING-SYSTEM: STUDY OF THE SYSTEM'S MAIN COMPONENTS

I.E. Saeed*, Zulkhairi Zainol Abidin

Department of Mech. & Manufacturing Eng., Faculty of Eng. & Built Environ., National University of Malaysia, 43600 Bangi, S.D.E., Malaysia.
****Corresponding author email: ismt5@yahoo.com***

ARTICLE DETAILS

Article History:

Received 23 June 2024
Revised 09 July 2024
Accepted 23 August 2024
Available online 26 August 2024

ABSTRACT

This part of the study on thermal analysis of solar-assisted drying-system**,** examined the thermal performance of the main components. Roselle is used as drying material for testing the drying-system. The silica gel is used to remove moisture from the drying-air before entering the drying-chamber. The research findings showed that the temperature and energy collected by the system increased with higher solar-irradiance levels. The solar collector had an average efficiency of 22%, and a time constant of 32 minutes. The average differences between the inlet and ambient temperatures, the outlet and inlet temperatures, and the inlet and ambient temperatures per unit of solar irradiance are 22.2°C, 1.5°C, and 0.04°Cm²/W, respectively.

KEYWORDS

thermal-investigation; solar-collector; heat-exchanger; water-tank; silica-gel; Roselle

1. INTRODUCTION

The increase in the world's population has led to a surge in energy demand, resulting in an escalated use of fossil fuels and a consequent rise in the prices (Barhoumi et al., 2020; Qusay et al., 2023). The utilization of renewable energy sources is increased in the recent years, as it is importance to concentrate on renewable energy sources to minimise the impacts of climate change (Chahartaghi et al., 2019; Qusay et al., 2023; Hassan, 2021). Sustainable infrastructure relies on these sources as a vital power, and various types are existing; including solar energy (Yasunaga et al., 2018; Bardineh et al., 2018; Ebhota and Tabakov, 2018). Solar energy is a renewable and environmentally friendly power source that is plentiful and inexhaustible (Luan and Phu, 2020). Solar thermal systems efficiently, harness a significant portion of the energy in shine hours (Sarbu and Sebarchievici, 2020).

Humans have been using drying as a way of preserving food for a long time. This process is the very important because it reduces the weight and volume of the food, which makes it easier to pack, store, and transport. It also allows the food to be stored at room temperature (Mujumdar, 1995; Sacilik, 2007). Drying food is notably energy-demanding and thus contributes substantially to carbon emissions. The food sector's greenhouse gas emissions account for approximately 30% of the total-emissions in the world (Hassan et al., 2023). As traditional energy sources become more expensive, polluting, and harmful to the environment, people are looking for cleaner and renewable alternatives (Buzas et al., 1998; Karsli, 2007). Reducing emissions from the food industry and waste is possible through proper preservation methods like drying with these alternatives (Hassan et al., 2023; Pham et al., 2020).

Solar dryers are one of these options, as they can dry food without using hot-air or direct sunlight (Sacilik, 2007; Pangavhane et al, 2002). The solar collector is a vital component of solar-heating systems; working as heat-exchanger (Duffie et al., 2020). It harnesses solar radiation, converts it to heat, and transfers this heat to a cooler medium, typically water or air. This energy serves various purposes (Rasha, 2020). Flat-plate solar collectors are distinguished for their capacity to absorb both direct and scattered solar radiation, offering the added benefit of low maintenance (Nazari et al., 2022).

The evaluation of the drying process involves both the drying material and system parameters. The thermal analysis of the components of the solar system begins with the basic step of assessing the performance of the solar collector. This involves exposing the collector to solar radiation and recording the temperatures of the fluid entering and exiting, along with the rate of fluid flow (Duffie et al., 2020). Collectors performance can then be characterized by the gained useful-energy, the thermal-efficiency of the solar-collector, and its heat-capacity (Akpinar et al., 2006; Kadam and Samuel, 2006; Azharul and Hawlader, 2006). The later reveals the collector's response characteristics under the transient or non-steady state (Hou et al., 2005).

Energy storage plays a crucial role in renewable-energy technology (Sarbu and Sebarchievici, 2020). To mitigate these intermittent effects, some researchers have suggested integrating solar dryers with thermal-energy storage-materials to store excess heat during the day for night-uses (Sari et al., 2015). The storage of solar-thermal-energy is indispensable; without it, solar energy must be utilized immediately upon receipt (Sameti et al., 2014; Adeyanju, 2015). Storage tanks primarily conserve hot-water for future use, to maintain continuous functionality, and to let the system operate effectively during periods of low/no solar radiation (Rasha, 2020; Beemkumar et al., 2017; Sarbu and Sebarchievici, 2020). They store thermal energy as sensible heat maintains a single-phase of the storage-medium throughout the process, and they bridge the gap between available energy-sources and requirements (Kumar and Singh, 2022; Chavan et al., 2022). Water storage-tank is characterized by energy-balance equations that measure the energy received from solar-collector, the energy delivered to the load, and the energy lost to the environment (Sukhatme, 2002).

Heat exchangers are equipment that allow heat-exchange between fluids that have different temperatures (Cüneyt, 2017). These devices enable effective heat transfer between two mediums, where heat moves from the

Quick Response Code	Access this article online	
	Website: www.actamechanicamalaysia.com	**DOI:** 10.26480/amm.01.2024.60.77

Cite the Article: I.E. Saeed, Zulkhairi Zainol Abidin (2024). Evaluation and Thermal-Analysis of A Solar-Assisted Drying-System: Study of The System's Main Components. *Acta Mechanica Malaysia, 7(1): 60-77.*

hotter fluid to the cooler fluid (Ismael and Kumari, 2014; Kushwah et al., 2017; Fernandes and Krishanmurthy, 2022). The transfer of heat takes place provided that the mediums are at different temperatures and in contact thermally (Mondal et al., 2014). The process is influenced by the system's temperature and the medium through which the heat is transferred (Nilay et al., 2017). The heat exchangers have various types, classifications, and constructions depending on their design and function (Zohuri, 2017). When analyzing heat exchangers, the overall-heat-transfer is expressed in terms of an average/mean temperature-difference of the two fluid streams (Fernandes and Krishanmurthy, 2022; Aijaz and Ravikumar, 2012). Additionally, the heat-capacity-rate ratio, the number-of-transfer-units (NTU), and the effectiveness can also be calculated (Kakac and Liu, 2002; Lienhard IV and Lienhard, 2008; Duffie et al., 2020; Aijaz and Ravikumar, 2012).

Energy supplied by the electric heater can be determined from the temperatures of the air at the inlet and outlet (Akpinar et al., 2006). The total energy input in solar-assisted drying is the summation of the energy provided by solar and auxiliary sources (Stehli and Escher, 1990). The incorporating a desiccant with solar systems leads to a significant decrease in energy consumption per kilogram of moisture removed (Chua and Chou, 2003). Furthermore, the moisture absorbed by the silica-gel can be determined from the break-through (concentration-time) curves (Chang et al.,2004). The aim of this part, of the work on the evaluation of a solar-assisted dehumidification-drying system, is to perform a general thermal analysis on main-components of the system. For the objective, thin-layer drying experiments are conducted using Roselle (*Hibiscus sabdariffa* L.), as a drying-material.

1.1 Mathematical modelling

The configuration and description of the system and its components are given in the Appendix.

1.2 Flat-plate solar collector

The gained useful-energy (Q_u) is given by (Luan and Phu, 2020; Duffie et al., 2020; Manglam et al. 2023, Aissaoui et al., 2016):

$$Q_u = A_c F_R[I_T(\tau\alpha) - U_L(T_i\ T_a)] = \dot{m}C_p(T_o\ \ T_i) \tag{1}$$

In the steady state, the instantaneous efficiency (η_i) is given by (Luan and Phu, 2020; Duffie et al. 2020; Kadam and Samuel, 2006; Wang et al.,2019; Aissaoui et al., 2016):

$$\eta_i = \frac{Q_u}{A_c I_T} = \frac{F_R[I_T(\tau\alpha) - U_L(T_i\ T_a)]}{I_T} = F_R(\tau\alpha)\ \ F_R U_L \frac{(T_i\ T_a)}{I_T} = \frac{\dot{m}\ C_p(T_o\ T_i)}{A_c I_T} \tag{2}$$

The heat-capacity is described in terms of a time constant, that is a time (t) at which the equality for following-equation (Eq.3) is reached (Hou et al., 2005; Duffie et al., 2020; Azharul and Hawlader, 2006):

$$(T_{o,t}\ \ T_i)/(\ T_{o,i}\ \ T_i) = 0.368 \tag{3}$$

1.3 Water storage tank

Considering the insulated water tank (Figure 1), that receives energy from solar-collector and discharges it to a load-drying (drying-chamber). Assuming a well-mixed liquid, at uniform temperature (T_l), which is varies only with time. Then, an energy-balance yields (Eq.4) (Kakac and Liu, 2002):

$$\left[(\rho VC_p)_l + (\rho VC_p)_t\right]\frac{dT_l}{dt} = q_u\ \ q_{load}\ \ \ (UA)_t(T_l\ T_a) \tag{4}$$

Denoting the sum of heat capacities $(\rho VCp)_l$ and $(\rho VCp)_t$ by $(\rho VCp)_e$, and integrating (Eq.4), under the assumption that q_u, q_{load}, & T_a are constant (with initial condition t=0, T_l=T_{li}), then (Eq.4) becomes:

$$\frac{q_u\ q_{load}\ (UA)_t(T_l\ T_a)}{q_u\ q_{load}\ (UA)_t(T_{li}\ T_a)} = exp\left[\ \frac{(UA)_t.t}{(\rho VC_p)_e}\right] \tag{5}$$

The assumption that q_u, q_{load}, and T_a are constant is valid if the time interval of the integration is kept small (≤1hr). The q_u and q_{load} is calculated from the inlet-temperature and outlet-temperature as (Yasunaga et al., 2018; Kant et al. 2016):

$$q_u = \dot{m}C_p(T_{fo}\ T_{fi}) = \dot{m}C_p(T_{fo}\ T_l) \tag{6}$$

$$q_{load} = \dot{m}_{load}C_p(T_l\ T_i) \tag{7}$$

$$q_{loss} = (UA)_t\ (T_l\ T_a) \tag{8}$$

Then (Eq.4) is written as:

$$(\rho VC_p)_e\frac{dT_l}{dt} = \dot{m}C_p(T_{fo}\ T_l)\ \dot{m}_{load}C_p(T_l\ T_i)\ (UA)_t(T_l\ T_a) \tag{9}$$

This (Eq.9) is used to determine the difference of temperature (T_l) with time, if the variation of q_u and (q_{load}) is given. The overall-heat transfer-coefficient (U_1) for the heat-flow through the cylindrical surface is given by:

$$\frac{1}{U_1} = \frac{r_1}{k_i}.ln\frac{r_2}{r_1} \tag{10}$$

Similarly, the overall-heat transfer-coefficient U_2 for the heat-flow through the flat surface is:

$$U_2 = k/\gamma \tag{11}$$

The term $(UA)_t$, (in WK^{-1}), is stated as:

$$(UA)_t = (U_1.\pi.\phi.H_t) + (U_2.2(\pi/4).\phi^2) \tag{12}$$

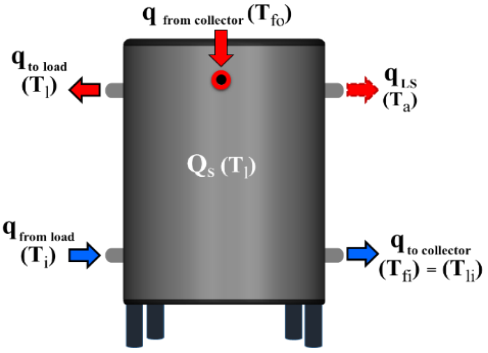

Figure 1: Water-tank: energy-balance

1.4 Heat exchangers

Overall heat-transfer is given by a mean-temperature difference between the two fluid-streams (T_{mean}), i.e., the logarithmic-mean-temperature difference ($LMTD$) (Fernandes and Krishanmurthy 2022; Zohuri, 2017; Khayal, 2018). The rate of heat-transfer for hot (h) and cold (c) streams can be given as (Cüneyt, 2017; Zhao et al., 2022):

$$Q_h = (\dot{m}c_p)_h(T_{h_{in}}\ T_{h_{out}}) = \qquad Q_c = (\dot{m}c_p)_c(T_{c_{out}}\ T_{c_{in}}) \tag{13}$$

Difference between the Q_h and Q_c is minor, Q_{aver} =(Q_h+Q_c)/2, and Q is (Zohuri, 2017):

$$Q = UA\,\Delta T_{mean} \tag{14}$$

The integration of equation (14) for cross-flow such that (Kakac and Liu, 2002):

$$dQ = U(T_h\ T_c)dA \tag{15}$$

will produce an integrated-LMTD, as follows:

$$dQ = UA\,\Delta T_{mean} \tag{16}$$

The ΔT_{mean} can be determined analytically using the following quantities (Fernandes and Krishanmurthy, 2022; Zohuri, 2017; Chen et al., 2022):

$$\Delta T_{mean,cf} = \frac{(T_{h_{out}}\ T_{c_{in}}) - (T_{h_{in}}\ T_{c_{out}})}{ln(T_{h_{out}}\ T_{c_{in}})/(T_{h_{in}}\ T_{c_{out}})} \tag{17}$$

P, is the proportion of the actual heat-transferred to the one that could be transferred if the same cold-fluid temperature is raised to the hot-fluid inlet-temperature (it is the heat-exchanger's temperature effectiveness) (Cüneyt, 2017; Chen et al., 2022). The value of P ranges from 0-1.

$$P = \frac{(T_{c_{out}}\ T_{c_{in}})}{(T_{h_{in}}\ T_{c_{in}})} = \frac{\Delta T_{c_{out}}}{\Delta T_{max}} \tag{18}$$

R, is the proportion of ($\dot{m}C_p$) of cold-fluid to that of hot-fluid (≤1), (it is the heat-capacity rate-ratio) (Cüneyt, 2017; Chen et al., 2022):

$$R = \frac{(T_{h_{in}}\ T_{h_{out}})}{(T_{c_{out}}\ T_{c_{in}})} = \frac{C_c}{C_h} \tag{19}$$

Then, for cross flow (Cüneyt, 2017; Zohuri, 2017; Chen et al., 2022):

$$Q = U.A.F.\Delta T_{(mean\ cf)} \tag{20}$$

Where, F is a correction factor (-), (it depends on Temperature-Effectiveness-P, the heat-capacity rate-ratio R and the flow-arrangement), cf = cross flow. It is available in chart form (Lienhard and Lienhard, 2008). It is <1 for multi-pass and cross flow, and =1 for true counter-flow heat-exchangers. F measures the departure of the true-mean temperature from the $LMTD$ for a counter-flow-arrangement. R between zero-∞, and in case of negligible temperature variation of one fluid, P or R = zero, and F =1 (Cüneyt, 2017).

Heat-capacity rate-ratio (C*) (Cüneyt, 2017; Lienhard and Lienhard, 2008; Orozaliev et al., 2008):

$$C^* = C_{min}/C_{max} \tag{21}$$

Where, C_{min} and C_{max} are the smaller and the larger magnitudes of C_h and C_c (it is ≤1).

$$Q_{max} = (\dot{m}\, c_p)_c (T_{h_{in}} - T_{c_{in}}) \;\; if \; C_c < C_h$$

$$Q_{max} = (\dot{m}\, c_p)_h (T_{h_{in}} - T_{c_{in}}) \;\; if \; C_h < C_c$$

where $C_c=(\dot{m}\, c_p)_c$ and $C_h=(\dot{m}\, c_p)_h$ are respectively, the heat-capacity-rates of cold and hot fluids, $\dot{m}$ is mass-flow-rate, and c_p is specific-heat (Cüneyt, 2017).

Effectiveness of heat exchanger (ε): It measures the actual-heat transferred divided by maximum one that could possibly be done from one stream to the other (Duffie et al., 2020; Azharul Karim and Hawlader, 2006; Cüneyt, 2017; Kakac and Liu, 2002). This is given as (Khayal, 2018; Raju et al., 2014):

$$\varepsilon = \frac{Q}{Q_{max}} = \frac{C_h(T_{h_{in}} T_{h_{out}})}{C_{min}(T_{h_{in}} T_{c_{in}})} = \frac{C_c(T_{c_{out}} T_{c_{in}})}{C_{min}(T_{h_{in}} T_{c_{in}})} \tag{22}$$

Where, C_{min} = the-smaller of C_c and C_h, i.e., the first definition is for $C_h = C_{min}$, and the second one is for $C_c = C_{min}$. ε is range as 0-1. Tables representing the relations between F, P, and R is given by (Cüneyt, 2017).

1.5 Electric heater output (Akpinar et al., 2006):

$$Q_{gda} = m_{da}\, C_{p,d_a}(T_o\; T_i) \tag{23}$$

1.6 Solar fraction (f) from total-energy (Duffie et al., 2020):

$$f = (Q_{load} \;\; Q_{auxillary})/Q_{load} = Q_{solar}/Q_{load} \tag{24}$$

1.7 Overall energy input in solar-assisted drying (Stehli and Escher, 1990):

$$Q_{tot} = Q_c + Q_e \tag{25}$$

1.8 Moisture-uptakes on the silica gel (q_m): It is estimated from the breakthrough (concentration-time) as follows (Chang et al., 2004; Tao et al., 2004):

$$q_w = \frac{F.\rho_{A0}.C_0}{W} \int_0^\infty \left(1 \; \frac{C_E}{C_0}\right) dt \tag{26}$$

2. Results and Discussions

Thin-layer solar drying experiments are conducted in solar-dehumidification drying-system. Roselle (Karkade) is used as drying material. The solar-drying experiments are continued (day-night), as an auxiliary electric-heaters are provided. The drying is carried out at different temperatures (35-65°C), and air flow-rates (1.5 and 3ms^{-1}). The temperatures and solar-irradiance values are averaged for every 15 minutes and plotted on one-hour intervals. Figure 2 showed the ambient, collector inlet & outlet temperatures, and solar irradiance, variation during the drying-experiments (Sari et al., 2015).

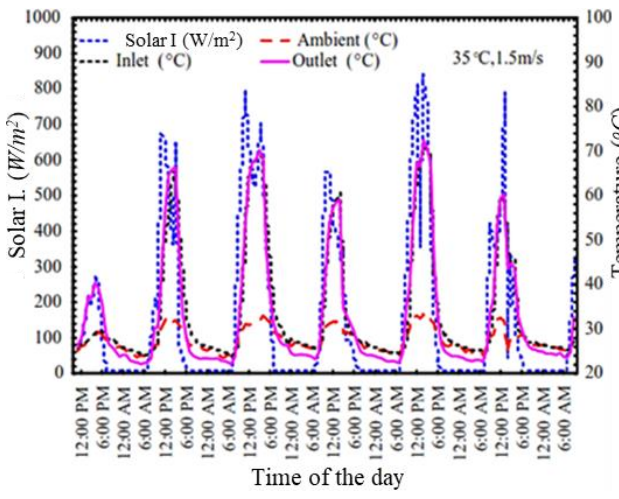

a: 35°C, 1.5m/s

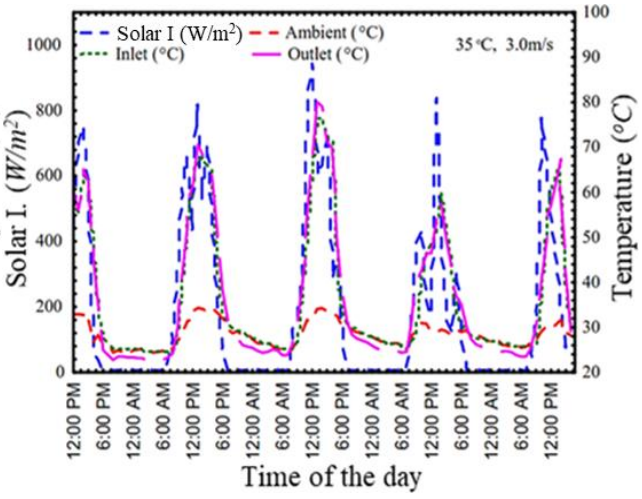

b: 35°C, 3m/s

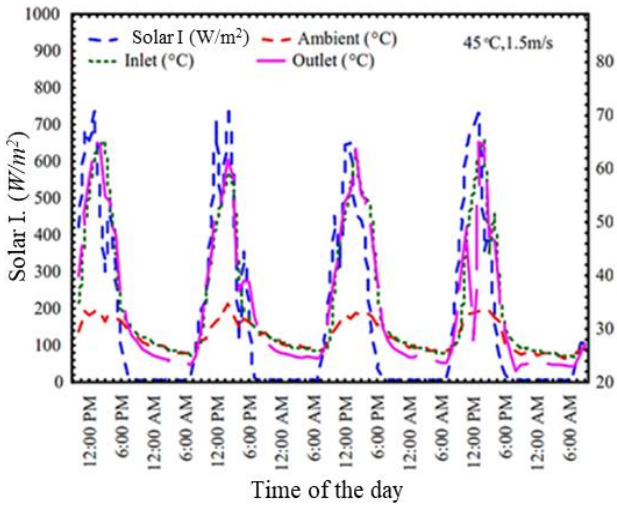

c: 45°C, 1.5m/s

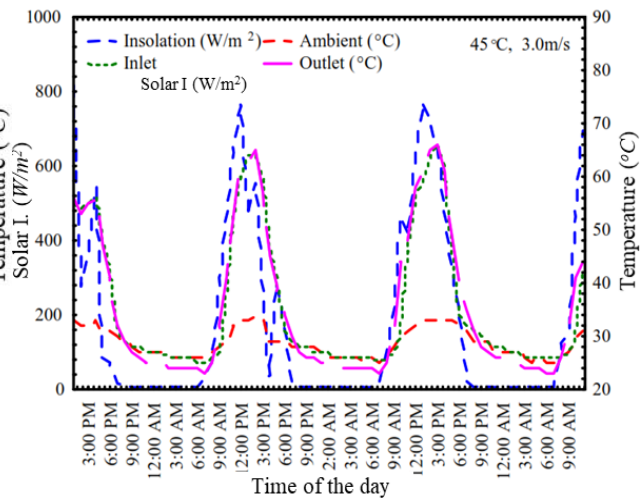

d: 45°C, 3m/s

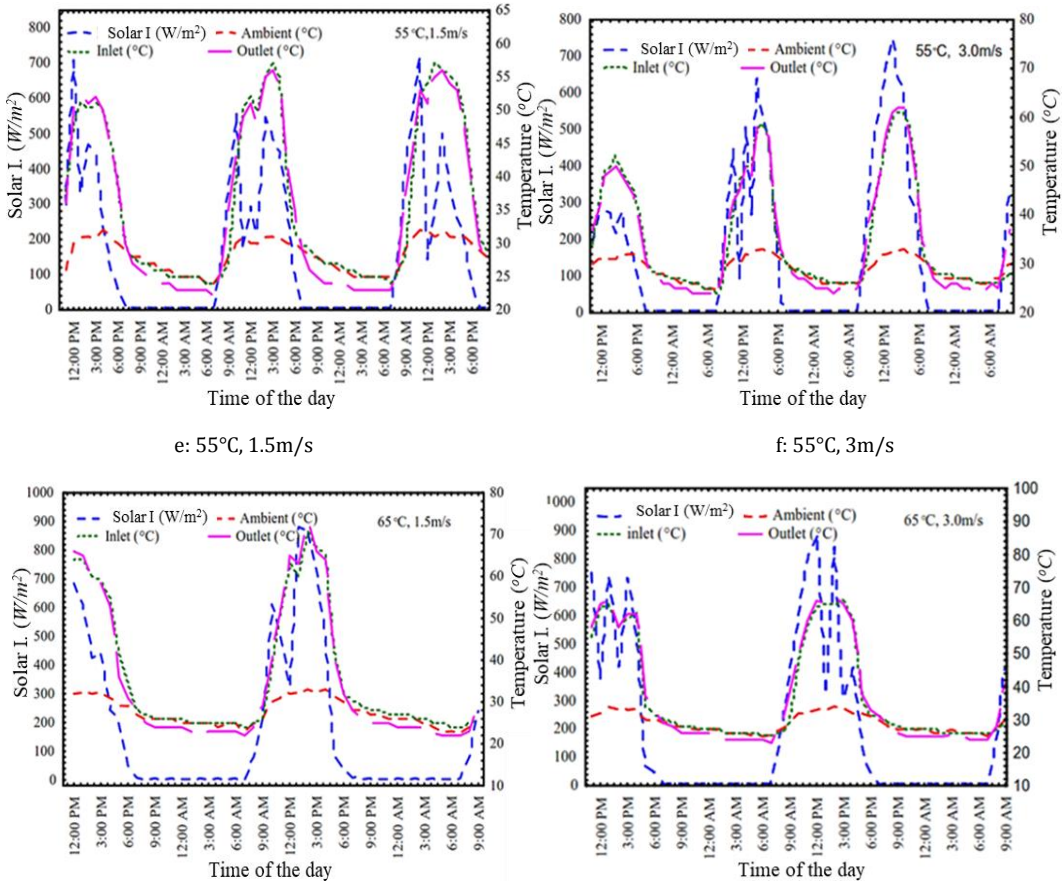

e: 55°C, 1.5m/s

f: 55°C, 3m/s

g: 65°C, 1.5m/s

h: 65°C, 3m/s

Figure 2: Temperatures (ambient, collector inlet & outlet) and irradiance vs. Time

As it shown in the Figure, higher temperatures occurred at higher irradiance levels. The peak values of the temperatures and irradiance are recorded around the mid of the day, as the drying time are varied between 1.92 to 5.95 days, for drying at 65 and 35°C, respectively. Figure 3 presented variations of the ambient, collector's outlet, and drying chamber inlet-temperature and outlet-temperature. At high irradiance levels, higher temperatures are achieved at the collect's outlet, in addition to ambient temperature. For drying at low temperature (35-45°C) the energy supplied by the collector is exceeded the drying load, while in drying at higher temperature (55-65°C), the drying-load is achieved around the mid-day-time only and the auxiliary heater is put-on repeatedly.

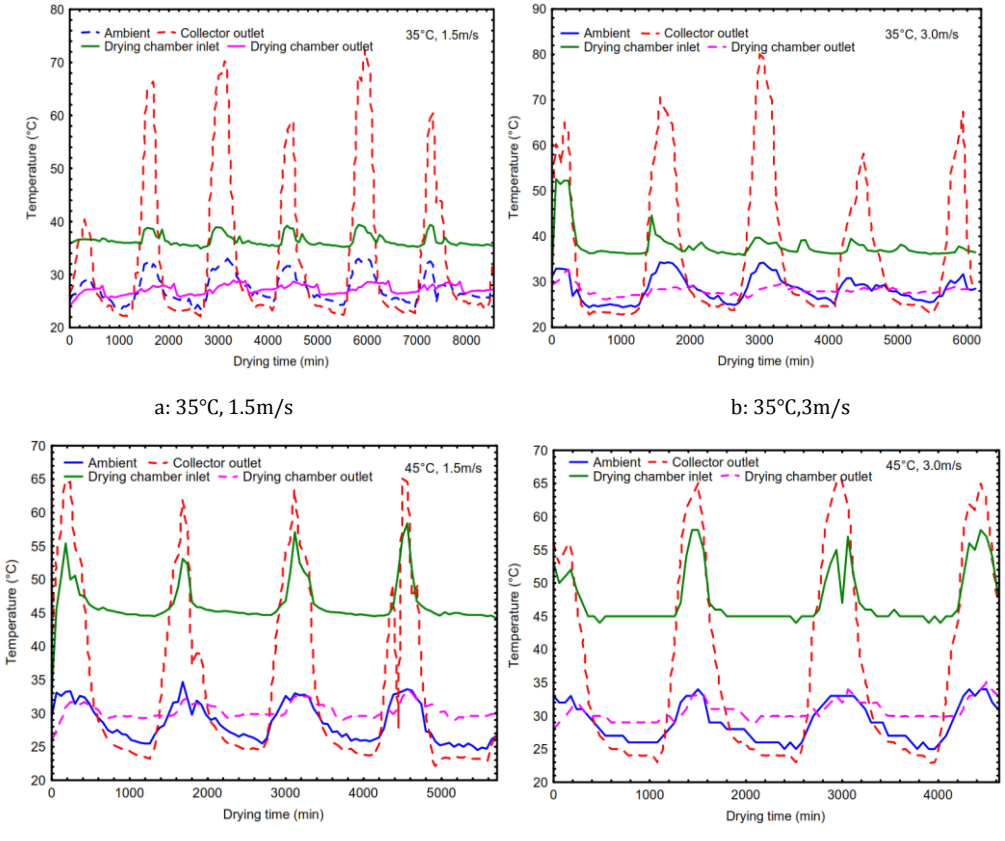

a: 35°C, 1.5m/s

b: 35°C,3m/s

c: 45°C, 1.5m/s

d: 45°C, 3m/s

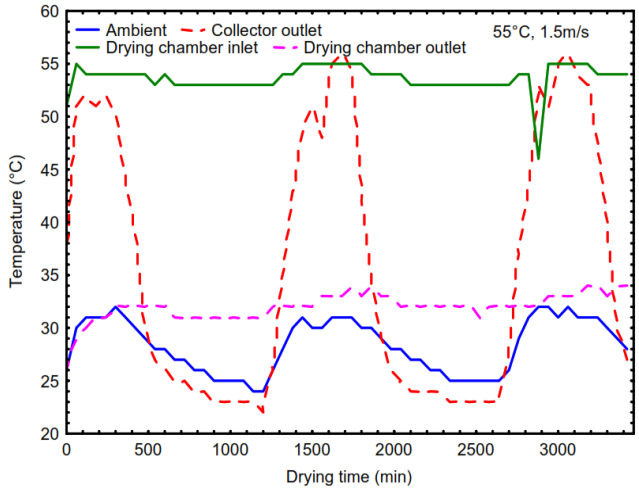

e: 55°C, 1.5m/s

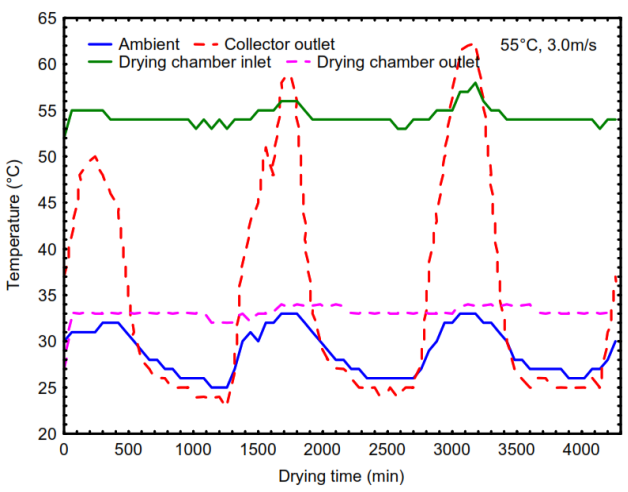

f: 55°C, 3m/s

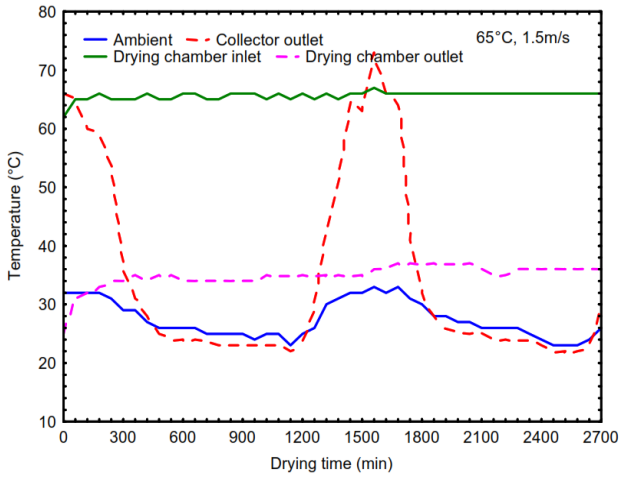

g: 65°C, 1.5m/s

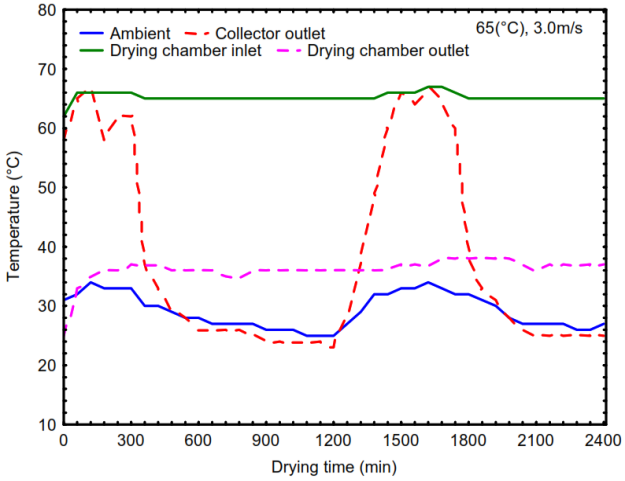

h: 65°C, 3m/s

Figure 3: Temperature (ambient, collector outlet, chamber inlet and outlet) vs. Time

Collector efficiency is a single parameter that combines collector and system characteristics. For most of the time, the collector's efficiency is less than 50%, which is owing to the reason that the collector is operated at high temperatures. These high temperatures are reached because the stored water is about 100 litres and the collector area is ≈10m² (ratio of 10:1). For general use an approximate thumb rule for fixing the storage-tank size is to use about 75 to 100 litre of storage/m² of the collector surface, ≈ ratio of 100:1 (Sukhatme, 2002). For household hot-water, some researchers used collector area of 18 m^2 and a storage tank of 31 m^3, with a volume-to-area ratio of 1.72 ((Rabbani and Tariq, 2019).

It is worthy to show the variations of the instantaneous collector's efficiency, with the time of the day, as well as the outlet temperature, and solar irradiance, as given in Figure 4. In their study on air-collector, showed that the thermal-efficiency is influenced by the intensity of sunlight, with the highest efficiency observed at a solar intensity of 750W/m², and beyond this point, the efficiency declined sharply (Kadam and Samuel, 2006; Azharul and Hawlader, 2006; Condori et al., 2001; Carmona et al., 2017; Rahul et al., 2023). A group researchers tested flat-plate-collector with storage, and found average efficiency values of 24.3%, 27.4%, and 24.5%, for month of Oct., Dec., and Feb., respectively (Carmona et al., 2017).

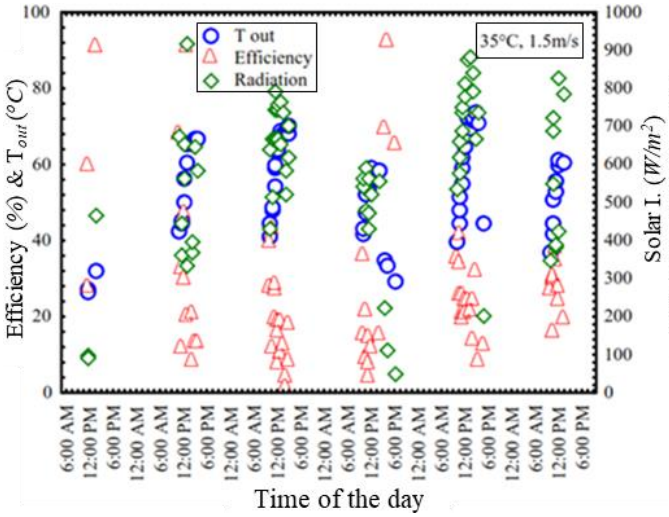

a: 35°C, 1.5m/s

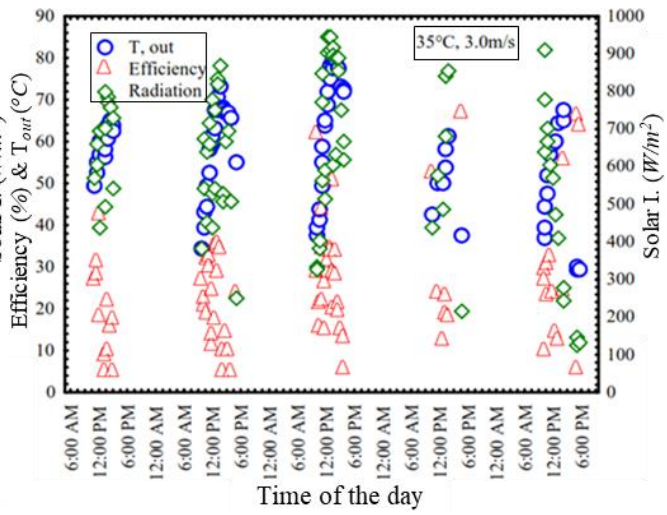

b: 35°C, 3m/s

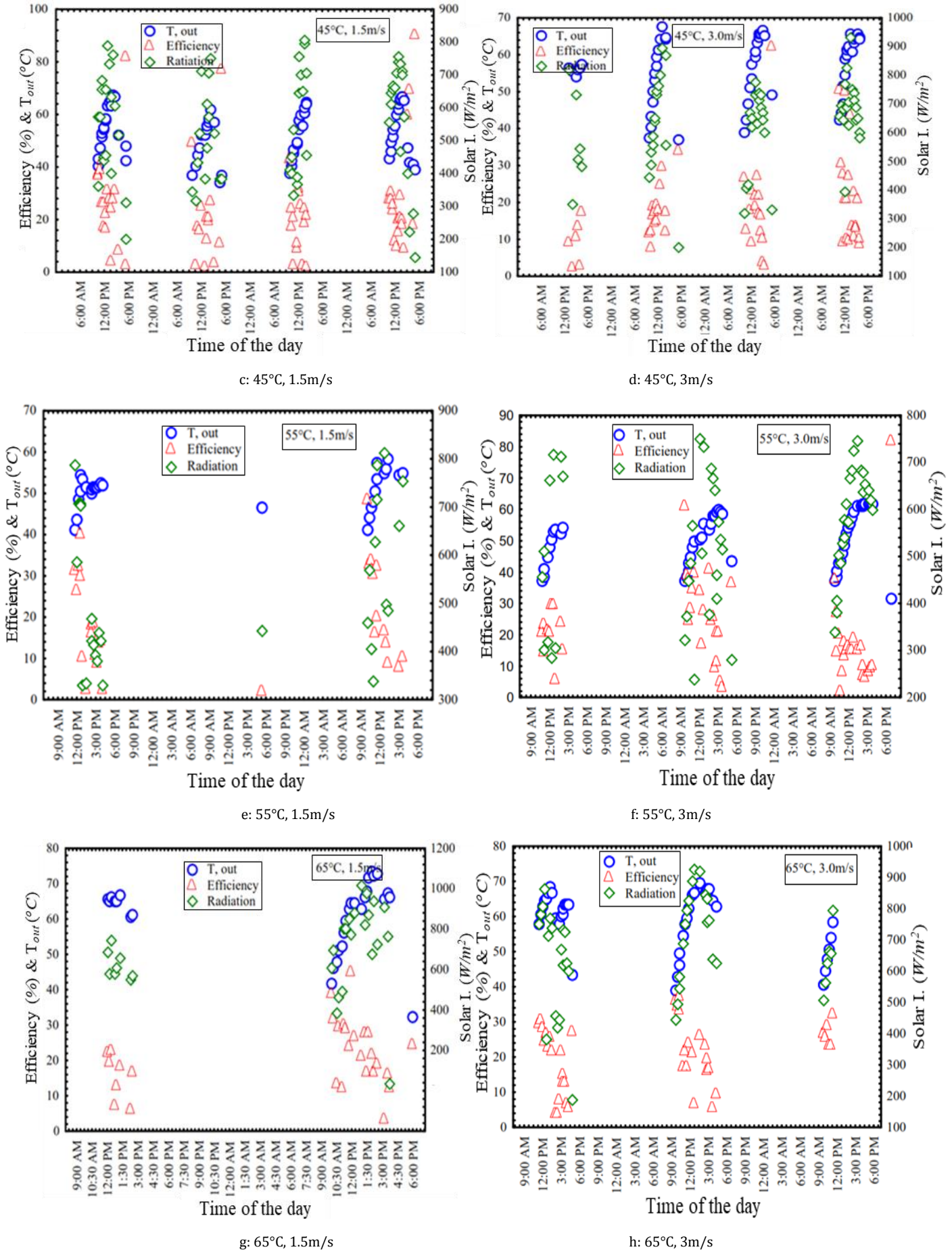

c: 45°C, 1.5m/s

d: 45°C, 3m/s

e: 55°C, 1.5m/s

f: 55°C, 3m/s

g: 65°C, 1.5m/s

h: 65°C, 3m/s

Figure 4: Efficiency, collector (T_{out}) and irradiance vs. Time of day

The temperature difference (T_i-T_a) values are varied according to the levels of the received-irradiance on the collector's surface. The maximum value is 43.5°C. A typical range of 10-60°C, for single-glazed collector, is presented by (Buzas et al., 1998). The relationship is given in Figure 5. Linear-fit is done, and the correlation coefficient (r^2) is given. The values of r^2 are not high because the solar irradiance varied-greatly (cloudy-sky), and hence, the fit is moderate or low (Condori et al., 2001; Kadam and Samuel, 2006).

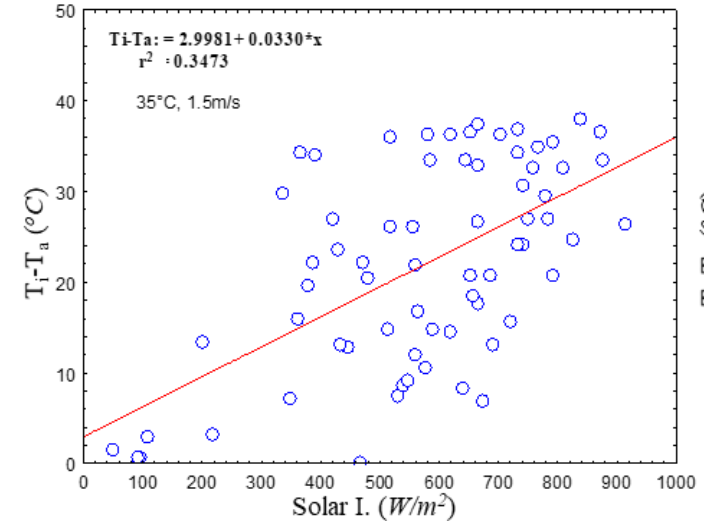

a: 35°C, 1.5m/s

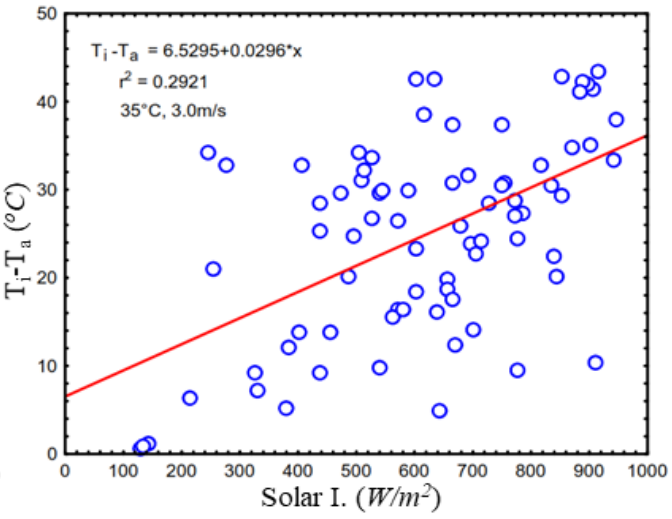

b: 35°C, 1.5m/s

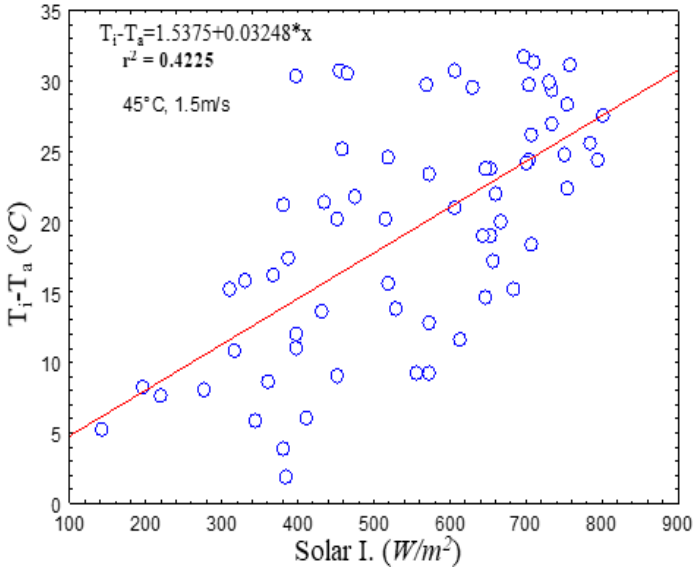

c: 45°C, 1.5m/s

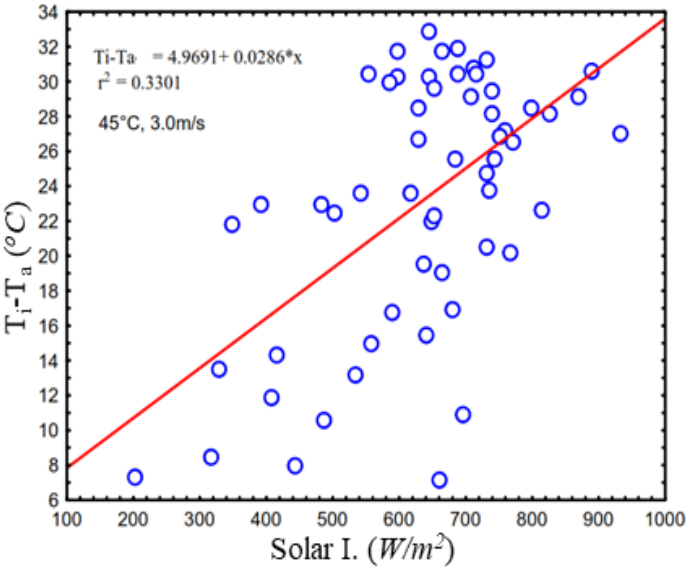

d: 45°C, 3m/s

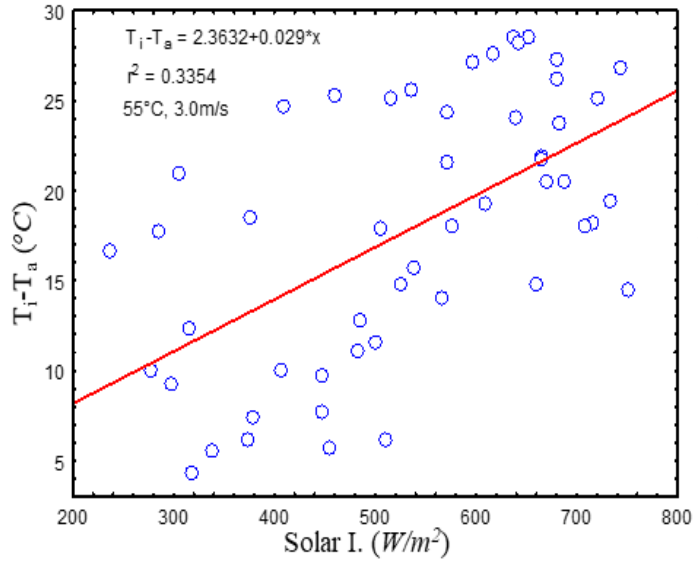

e: 55°C, 3.0m/s

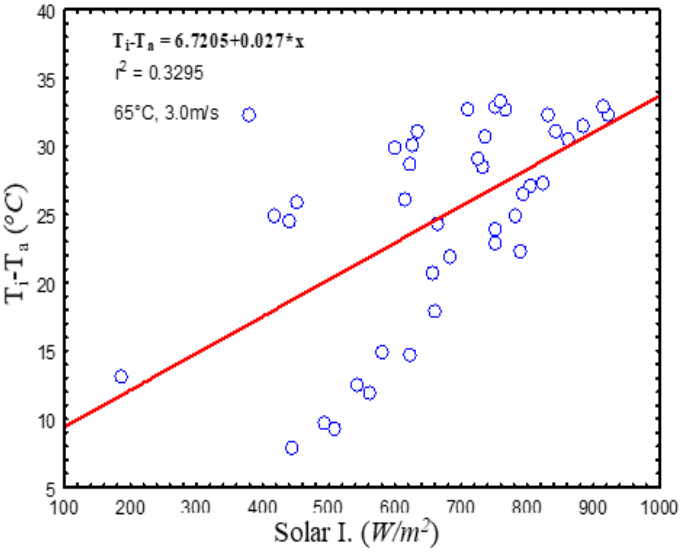

f: 65°C, 3.0m/s

Figure 5: Temperature (T_i-Ta) vs. Solar irradiance

Figure 6 presented the temperature differences between outlet and inlet of the collector (T_o-T_i) at different solar intensities. The differences are increased at higher irradiance levels, and the maximum value is 5.4°C. Linear-correlation of ΔT with solar irradiance (which is diverse), is done. The analysis revealed a moderate fit. Similar result is shown by (Kadam and Samuel, 2006), where they found (T_o-T_a = 0.0038*I+5.3442), with R^2 =(0.0596).

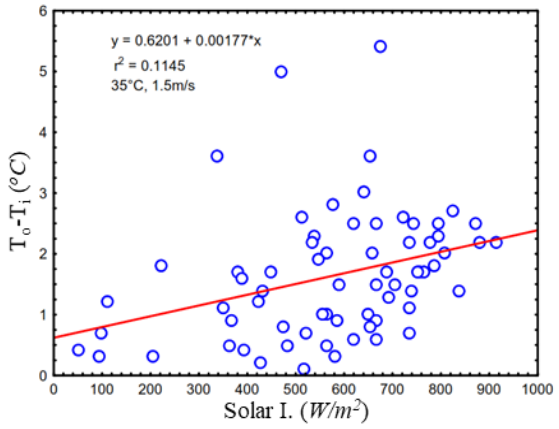

a: 35°C, 1.5m/s

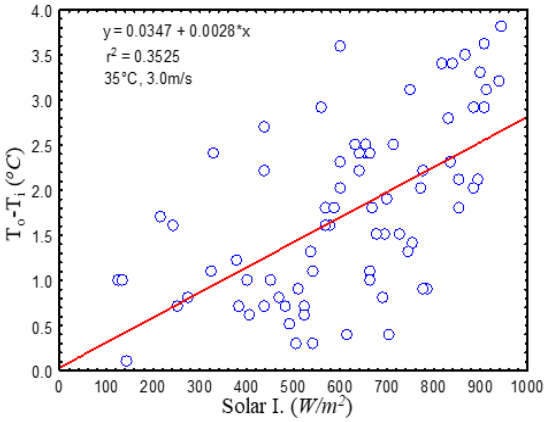

b: 35°C, 3m/s

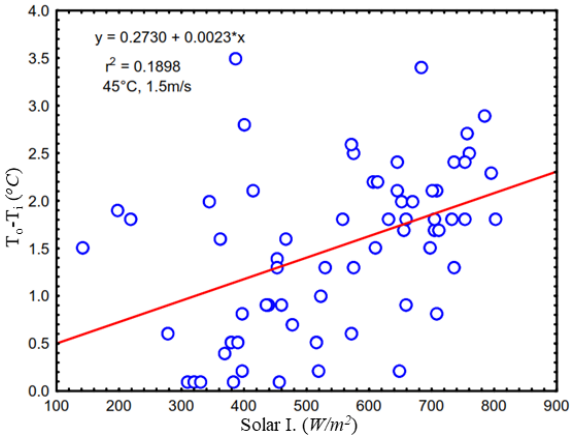

c: 45°C, 1.5m/s

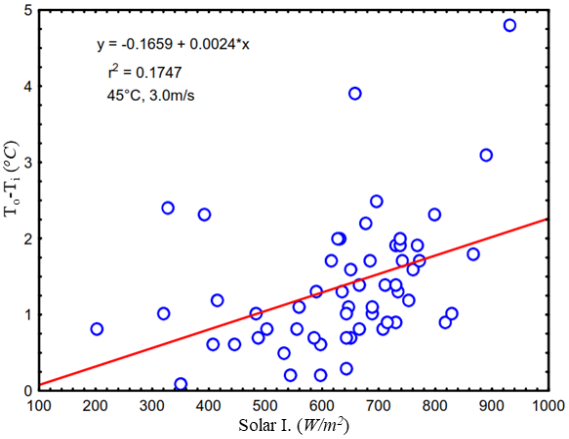

d: 45°C, 3m/s

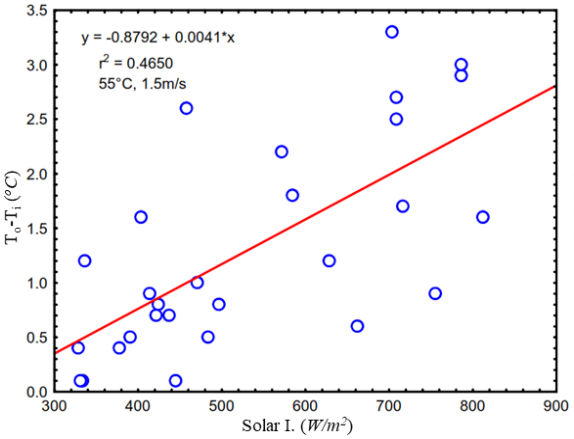

e: 55°C, 1.5m/s

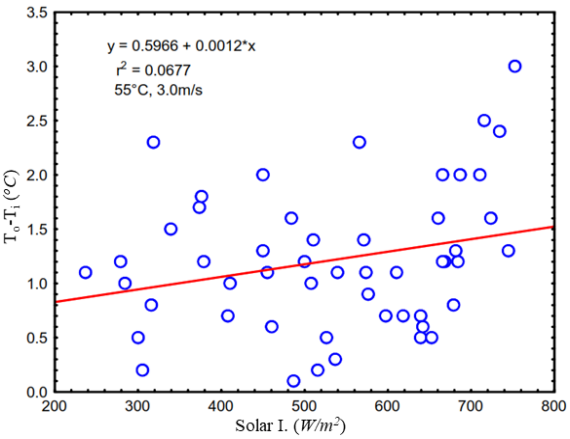

f: 55°C, 3m/s

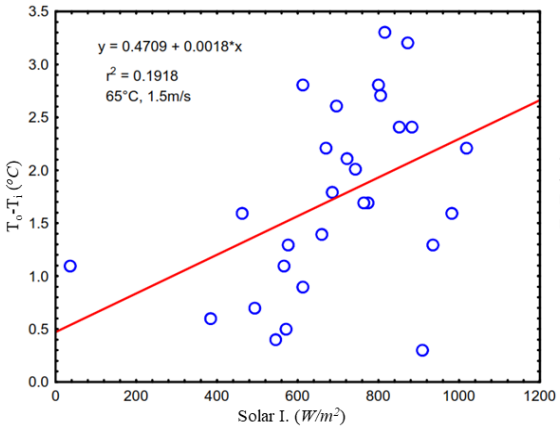

g: 65°C, 1.5m/s

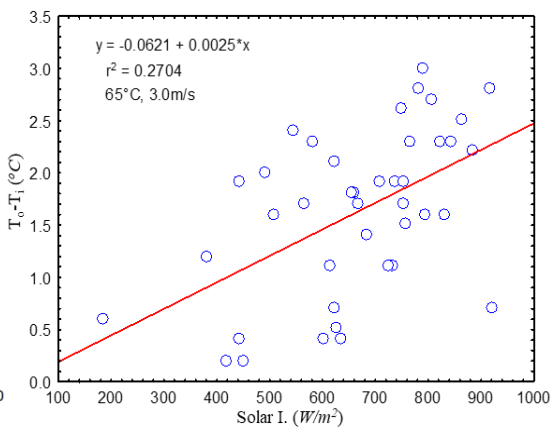

h: 65°C, 3.0m/s

Figure 6: Temperature (T_o-T_i) vs. Solar irradiance

The solar-collector performance is highly reliant on the environmental factors, as solar-irradiance, ambient-temperature and relative-humidity (Kadam and Samuel, 2006). It is apparent as of Figure 7 that the energy-output of the collector ($Q_{collector}$) increment is directly affected by solar irradiance, where higher energy is collected at higher irradiance level.

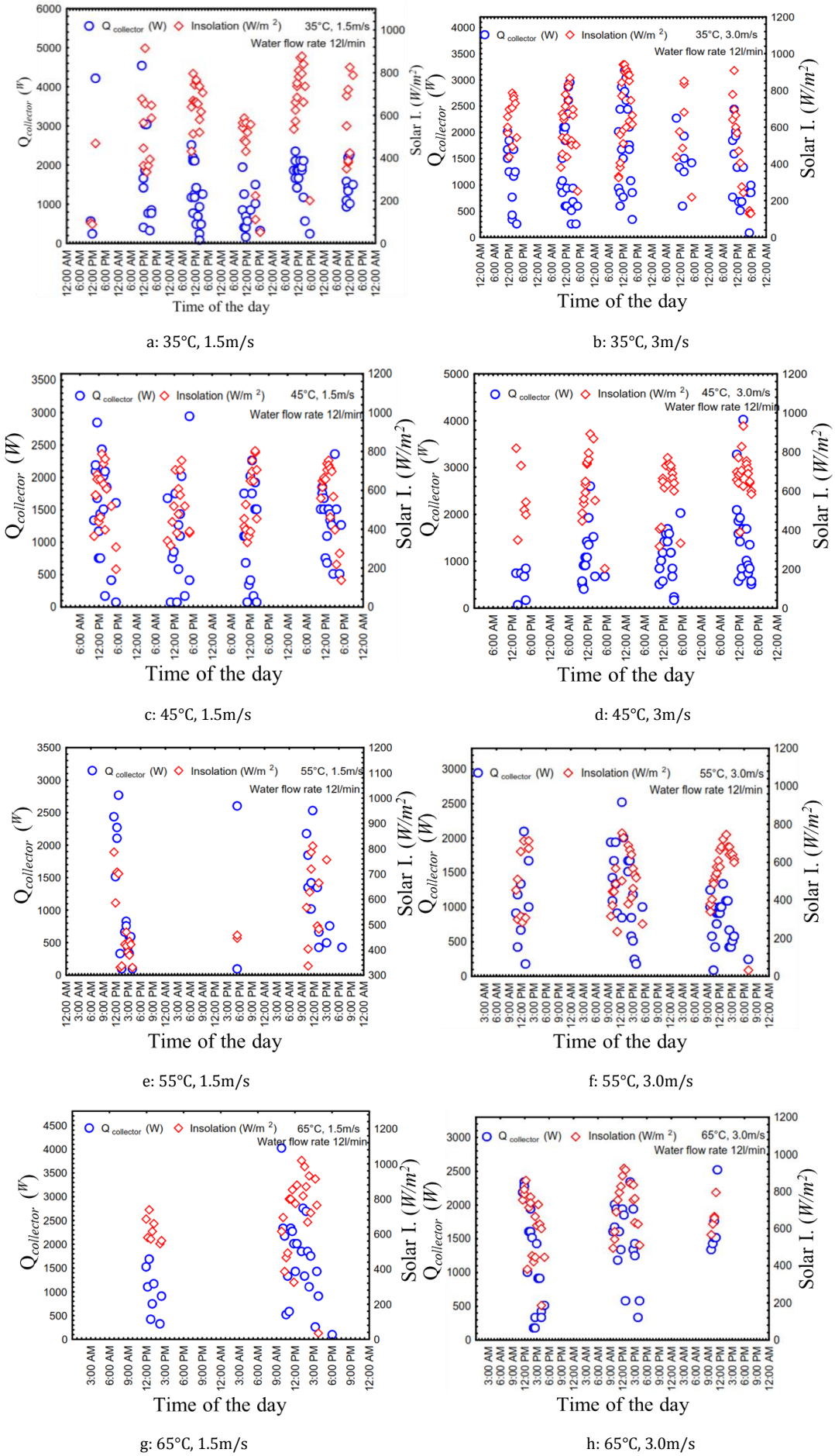

a: 35°C, 1.5m/s

b: 35°C, 3m/s

c: 45°C, 1.5m/s

d: 45°C, 3m/s

e: 55°C, 1.5m/s

f: 55°C, 3.0m/s

g: 65°C, 1.5m/s

h: 65°C, 3.0m/s

Figure 7: $Q_{collector}$ and irradiance vs. Time of day

The difference of the inlet-temperature and outlet-temperature of the silica-gel-columns, during the processes of dehumidification-regeneration, with drying time are presented in Figure 8. Each of the two silica gel columns is regenerated, at 60°C, for ≈12h/day, alternatively, and then used for dehumidification process. Moreover, the processes of dehumidification and regeneration are carried out simultaneously. The (zigzag) behaviour of the curves is resulted from shifting of the columns in the processes. The exit air-temperatures from both dehumidified and regenerated columns are greater than ambient-temperature (inlet-temperature for dehumidification). However, the later generates higher temperature, despite that the energies for condensation and evaporation nearly equal (as the regeneration temperature is 60°C). During dehumidification-process, the ambient-air temperature is increased after passing the silica gel column, as the water molecules gave-up their heat of condensation.

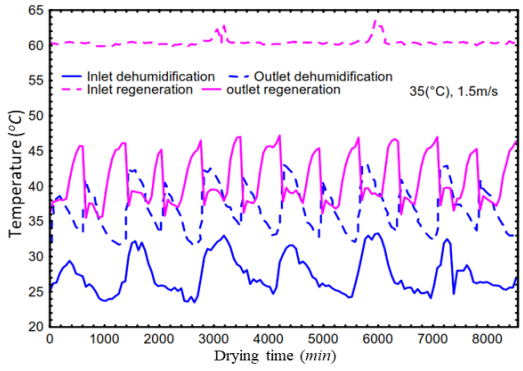

a: 35°C, 1.5m/s

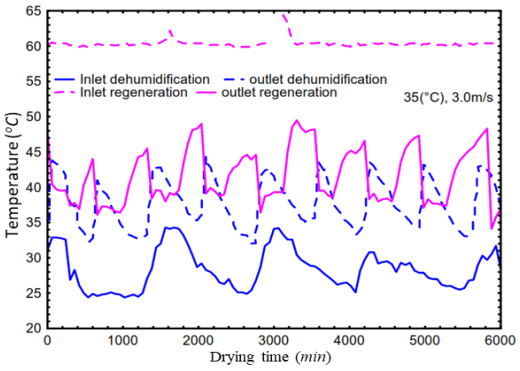

b: 35°C, 1.5m/s

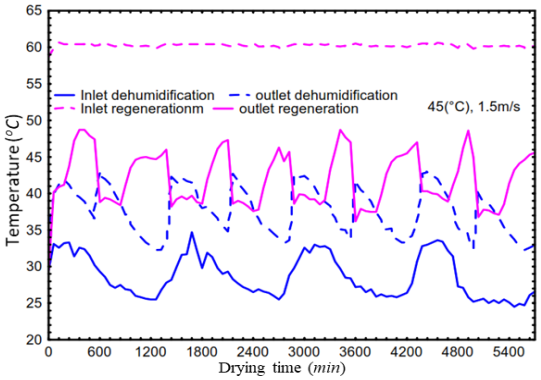

c: 45°C, 1.5m/s

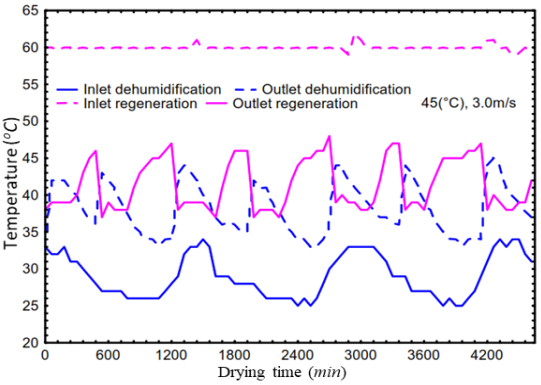

d: 45°C, 1.5m/s

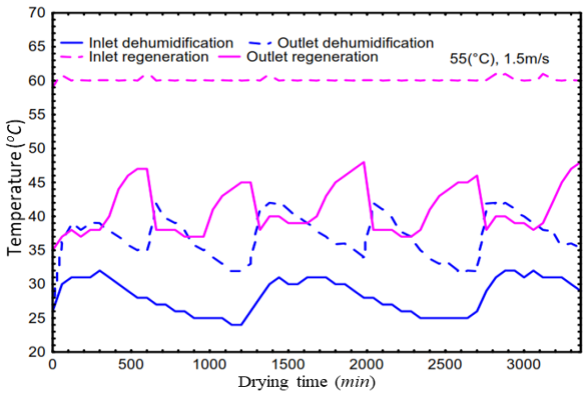

e: 55°C, 1.5m/s

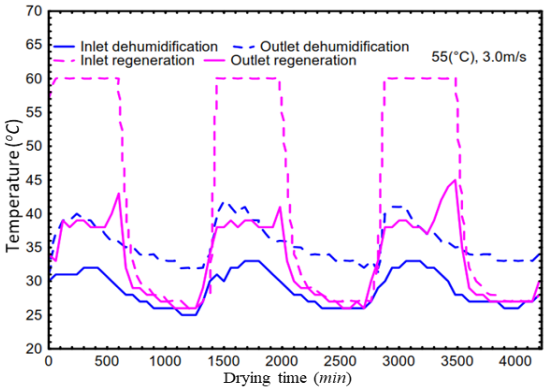

f: 55°C, 1.5m/s

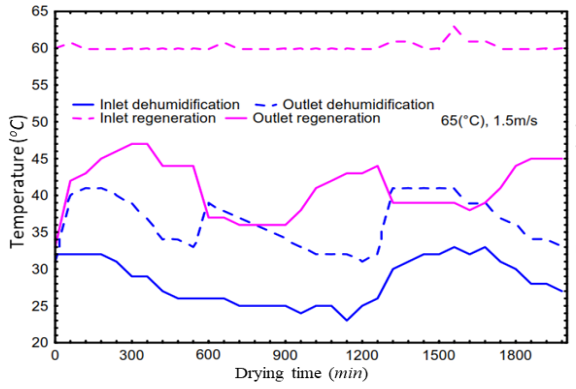

g: 65°C, 1.5m/s

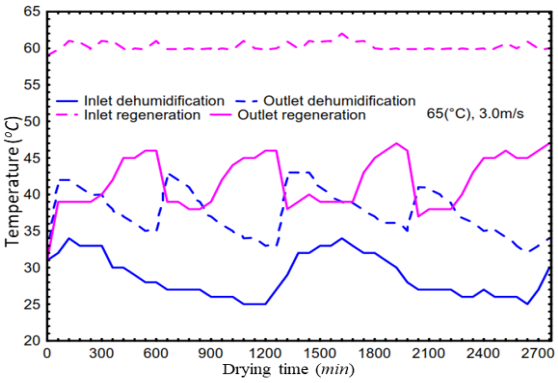

h: 65°C, 1.5m/s

Figure 8: Silica-gel columns inlet & outlet temperatures (dehum.- regeneration) vs. time

Figure 9 shows the ambient and water-storage-tank temperatures (measured at the centre of the tank), and energy losses from the tank versus time of day. Obviously, high losses are occurred during the daytime (max. around the mid-day time), where the tank received great amount of energy from the collector. At this time, the ambient temperature is also high. The minimum values of the heat losses are recorded after mid-night and near the morning time, as the tank continues to supply part of the energy to the drying-chamber for about 3-5hrs (depending on the drying temperature) after the collector has been stopped. The losses are also attributed to the water-tank size. The development of efficient and cost-effective thermal energy storage is of great significance as it bridges the gap between energy demand and supply (Reddy et al., 2015). A group researcher suggested a hot-water-tank design using principle of source-sink-matching (Zhang et al., 2023).

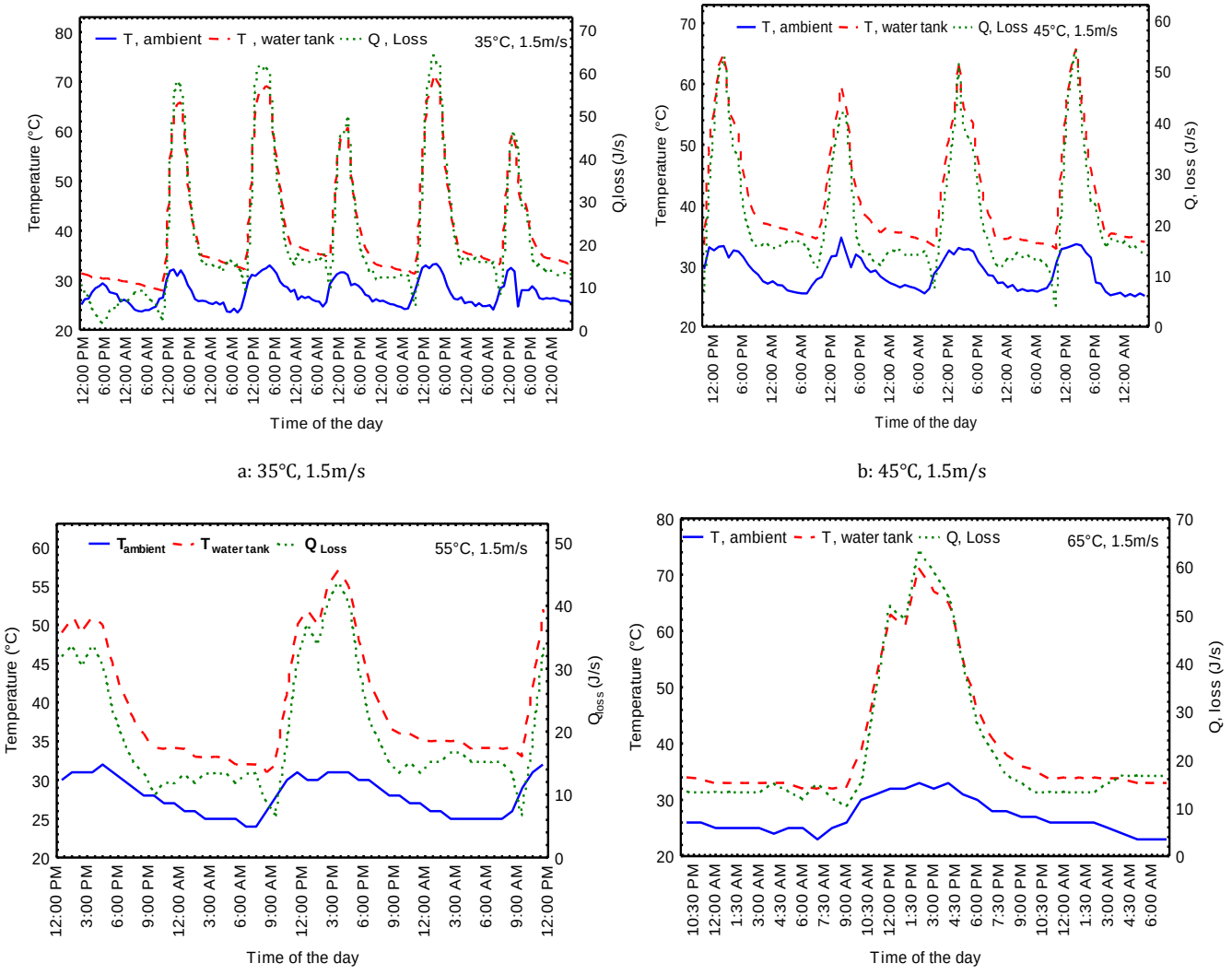

a: 35°C, 1.5m/s

b: 45°C, 1.5m/s

c: 55°C, 1.5m/s

d: 65°C, 1.5m/s

Figure 9: Ambient and water tank temperatures, and heat losses vs. time

Heat exchanger-1 (HE_1) is used for the regeneration of silica-gel. It receives hot water from the water tank via water pump-1 (WP_1) and transfers the energy to ambient air (which is forced by the blower-1 (B_1) to HE_1 and then to silica-gel). Figure 10 presented the variations of the energies carried by the hot water, supplied to the air, and the losses to environment. Higher losses are occurred when a great amount of energy is accumulated in the water tank, and then forced to the heat exchanger. Table1 showed the mean-temperature-difference (T_{mean}), the effectiveness, heat-capacity rate-ratio (*HCRR*), and heat losses (Q_{loss}).

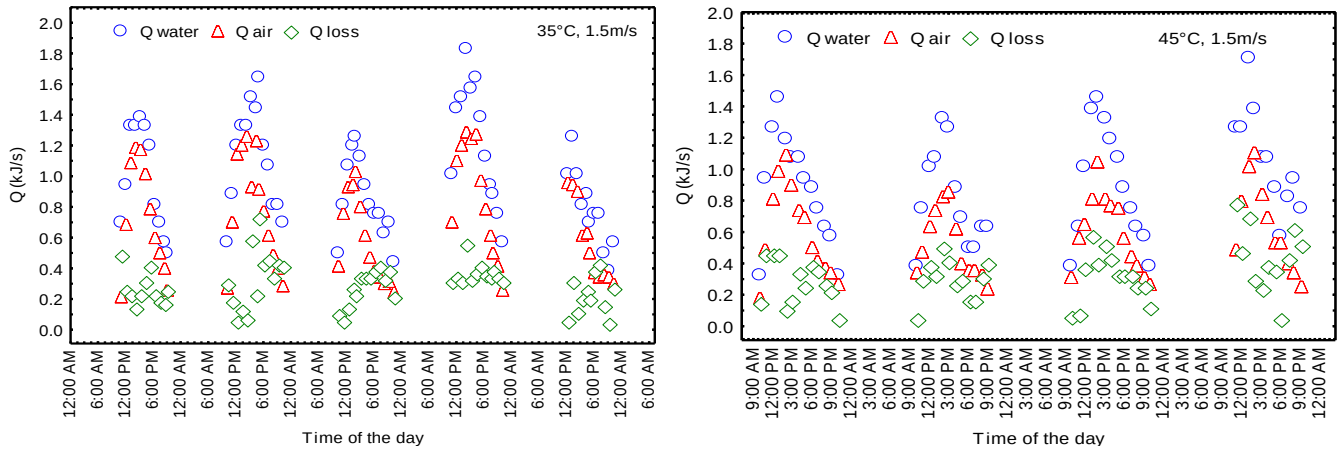

a: 35°C, 1.5m/s

b: 45°C, 1.5m/s

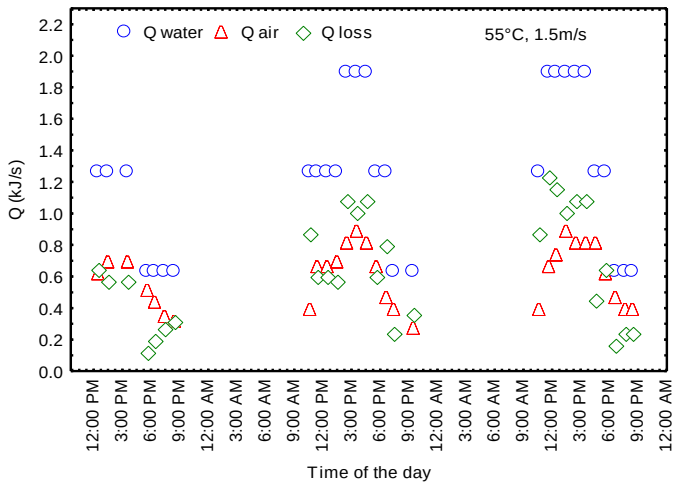

c: 55°C, 1.5m/s

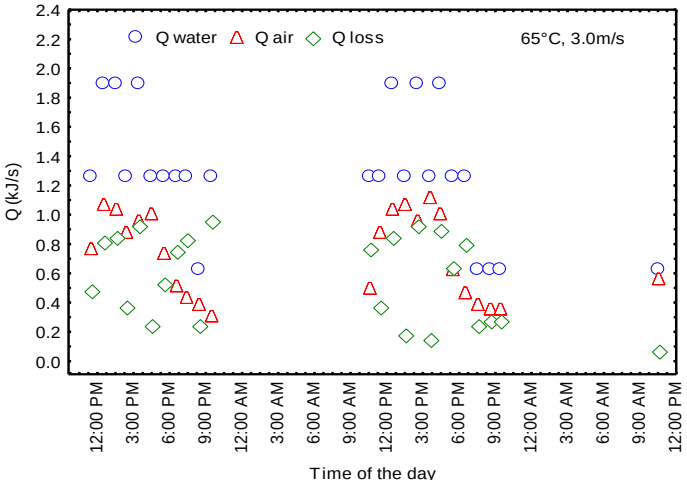

d: 65°C, 1.5m/s

Figure 10: HE_1, Q_w, Q_{air} and Q_{loss} vs. Time

Table 1: T_{mean}, effectiveness, HCRR, and Q_{loss}

Drying experiments			T_{mean} (°C)		Eff.ness		HCRR		Q (kJ.s^{-1})					
									Water		Air		Loss	
T	Vel.	Value												
°C	m/s	-	HE_1	HE_2	HE_1	HE_2	HE_1	HE_2	HE_1	HE_2	HE_1	HE_2	HE_1	HE_2
45	1.5	Aver	7	7	0.86	0.54	0.10	0.39	0.9	1.4	0.6	0.1	0.3	1.2
		Max	14	13	0.94	0.74	0.19	2.17	1.7	9.8	1.1	0.3	0.8	9.7
	3	Aver	8	7	0.87	0.58	0.80	0.11	0.8	0.7	0.7	0.3	0.2	0.4
		Max	22	16	0.95	0.80	0.17	0.50	1.9	4.4	1.2	0.6	1.2	3.9
55	1.5	Aver	8	7	0.85	0.64	0.13	0.20	1.2	0.9	0.6	0.1	0.6	0.8
		Max	13	10	0.92	0.76	0.20	0.50	1.9	1.3	0.9	0.2	1.2	1.2
	3	Aver	7	7	0.84	0.68	0.11	0.18	0.9	0.7	0.6	0.3	0.3	0.4
		Max	12	12	0.92	0.79	0.50	0.50	1.3	1.3	1.0	0.6	1.0	0.9
65	1.5	Aver	10	9	0.84	0.69	0.12	0.20	1.3	1.0	0.6	0.2	0.7	0.8
		Max	17	19	0.89	1.00	0.18	0.67	2.5	1.3	1.1	0.4	1.5	1.2
	3	Aver	9	9	0.85	0.71	0.12	0.16	1.3	1.0	0.7	0.4	0.6	0.6
		Max	16	15	0.91	0.79	0.25	0.50	1.9	1.9	1.1	0.7	1.0	1.3

Heat exchanger-2 (HE_2) is run for drying processes. It heats the dehumidified air (out of the silica-gel column) before ingoing the drying-chamber. Figure 11 showed the variations in the energy supplied (Q_w), transferred (Q_{air}), and lost to the surrounding (Q_{loss}). In drying at 35°C (1.5m/s and 3.0m/s), the heat-exchanger is not run. As the exit-air off the silica-gel column reached the drying temperature most of the time, and the auxiliary heater at the drying chamber's inlet, added small amount of energy when the temperature, of drying-air dropped below 35°C. The losses are high and many times exceeded the transferred amount of energy to the drying-air; as air velocities of 1.5m/s and 3.0m/s are used. However, more energy is carried by the air at higher velocity.

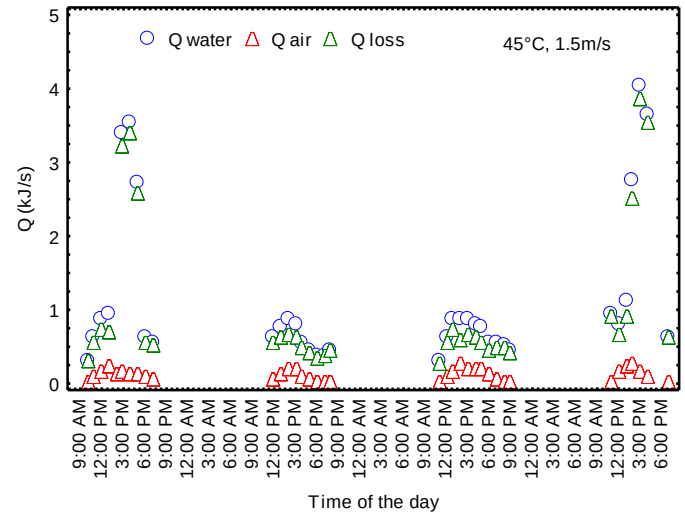

a: 45°C, 1.5m/s

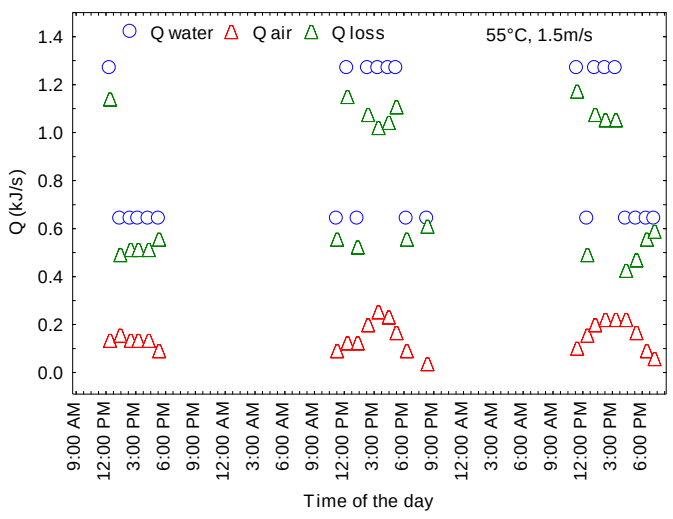

b: 55°C, 3.0m/s

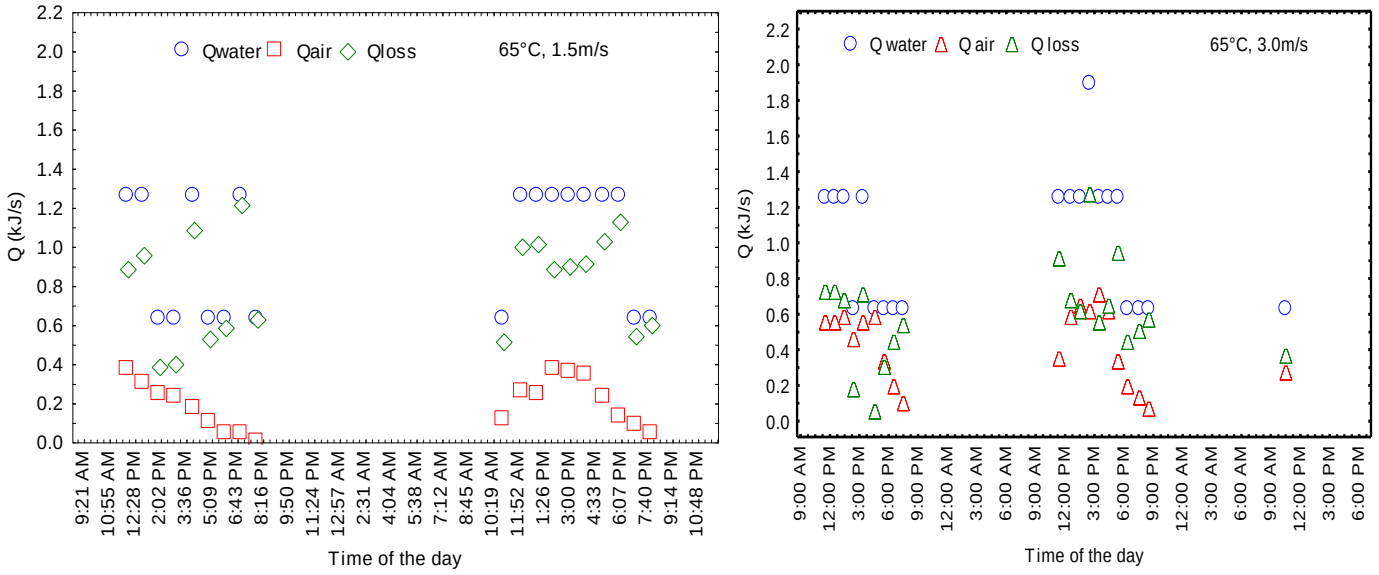

c: 65°C, 1.5m/s

d: 65°C, 3.0m/s

Figure 11: HE$_2$, Q$_w$, Q_{air} and Q_{loss} vs. Time

Heater-1 (H_1) is used for regeneration of silica-gel-columns at 60°C. The average energy consumed by this heater constituted 25% of the overall energy consumed in the system (Table 2). Figure 12 showed the energy supplied from H_1 ($Q_{heater1}$) and energy from solar (Q_{solar}) versus time of the day. The energy from the heater =zero, at the time the energy supplied by the solar-collector equal or exceeded the regeneration load (60°C).

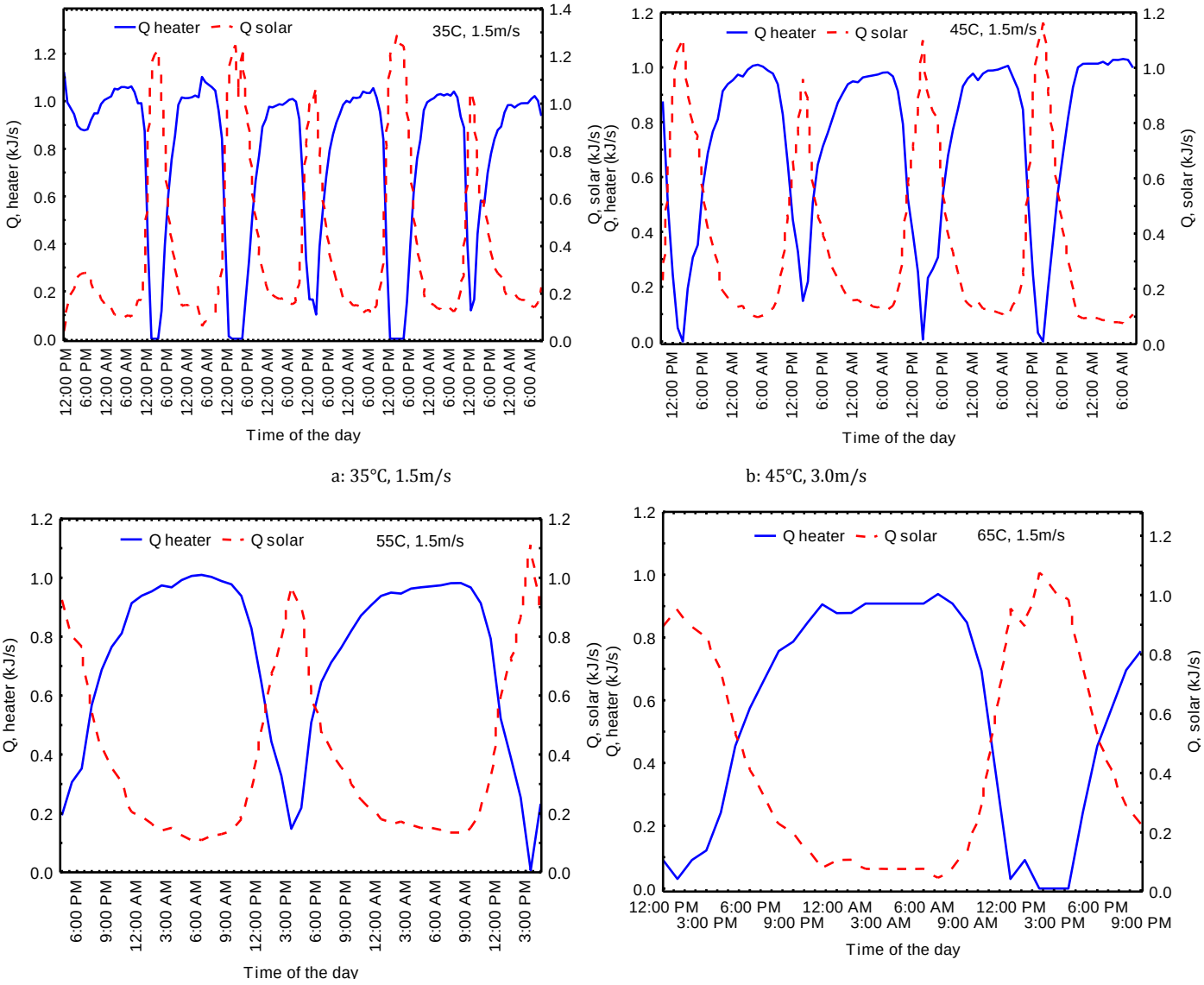

a: 35°C, 1.5m/s

b: 45°C, 3.0m/s

c: 55°C, 1.5m/s

d: 65°C, 1.5m/s

Figure 12: Q $_{heater1}$ and Q $_{solar}$ vs. Time of the day

Heater-2 (H_2) supplied energy for drying process, and it fixed at the inlet of the drying-chambers. The energy consumed by the heater ($Q_{heater2}$) constituted twelve percent of the energy consumed by the system (Table 2). Figure 13 showed the energy supplied from H_2 ($Q_{heater2}$) and energy from solar (Q_{solar}) versus time of the day. The energy output of the heater increased from 2kWh to 24kWh as the drying temperature is increase from 35°C to 65°C.

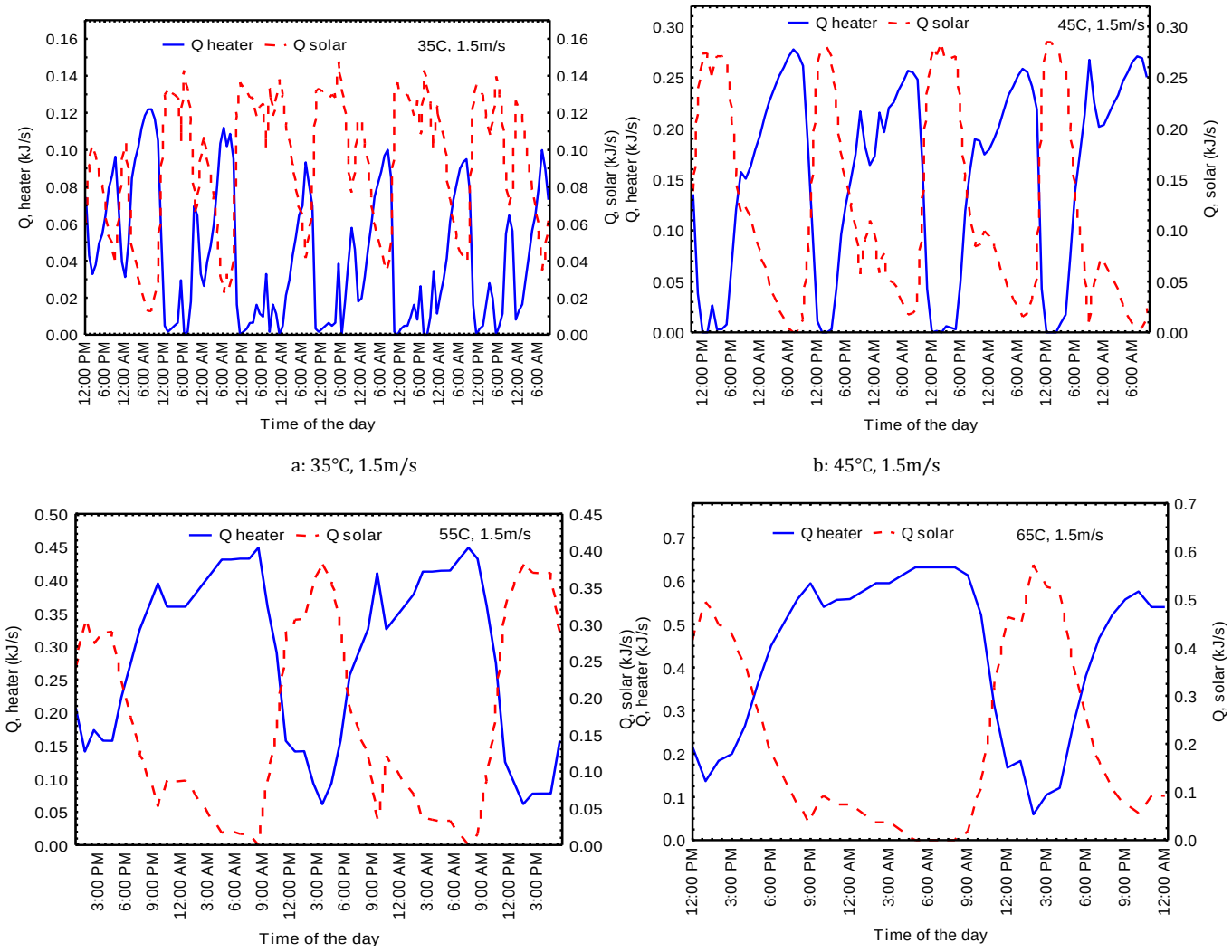

a: 35°C, 1.5m/s

b: 45°C, 1.5m/s

c: 55°C, 1.5m/s

d: 65°C, 1.5m/s

Figure 13: $Q_{heater2}$ and Q_{solar} vs. Time of the day

Water pumps play an essential role in solar-water heating-systems, circulating hot water from the collector to the water storage-tank. Centrifugal pumps are commonly employed in most solar systems (Rasha, 2020). The energy used for water pumping (P_1+P_2) and air blowers (B_1+B_2) are given in Table 2. They are also presented as percentage of the overall energy usage. The blowers constituted the largest part of the total-energy consumption (33%), while the water pumps used only 5%. Some researchers found that, at a mass-flow-rate of 0.041kg/s, the fan-power consumption is reduced by 16% compared to a rate of 0.061kg/s (Hassan et al., 2023).

Table 2: Q_{load}, $Q_{electricity}$, Q_{solar}, and solar fraction (f)

Drying experiments			Q *load* (kWh)					% Of the total Q *load*					
Temp.	Air velocity	Time	Q *electricity*			Q *solar*	Total	Q *electricity*					Q *Solar*
(°C)	(ms^{-1})	Hrs	H_{1+2}	P_{1+2}	B_{1+2}			H_1	H_2	P_{1+2}	B_{1+2}	Total *elec.*	*f*
35	1.5	143	186	16	122	48	372	39	2	5	38	84	16
	3.0	103	127	12	106	81	326	16	2	5	43	67	33
45	1.5	96	132	14	81	35	262	35	8	6	36	85	15
	3.0	78	129	12	80	51	272	28	7	6	36	77	23
55	1.5	58	91	5.6	49	21	167	34	14	4	34	85	15
	3.0	72	141	5.8	47	89	283	9	18	3	24	54	46
65	1.5	46	82	6.7	31	29	149	20	24	6	26	75	25
	3.0	48	111	7.6	51	41	211	22	20	4	30	76	24
Average		81	125	10	71	50	255	25	12	5	33	75	25
Max.		143	186	16	122	89	372	39	24	6	43	85	46
Min.		46	82	06	31	21	149	9	2	3	24	54	15

The moisture uptake on silica-gel is greatly-reliant on the degree of the regeneration of the column, humidity and velocity of the inlet-air (ambient-air), and regeneration time. The silica gel has relatively low regeneration-temperature, it is regenerated at 60°C, with average air velocity of 3.25m/s (Brundrett, 1987). Regenerating the columns takes long-time, which increased the power consumption. Consequently, the drying and thermal efficiencies are not high. Figure 14 presented the moisture uptake (*MU*) on the silica-gel; expressed as ($g_w.kg_{s.gel}^{-1}$).

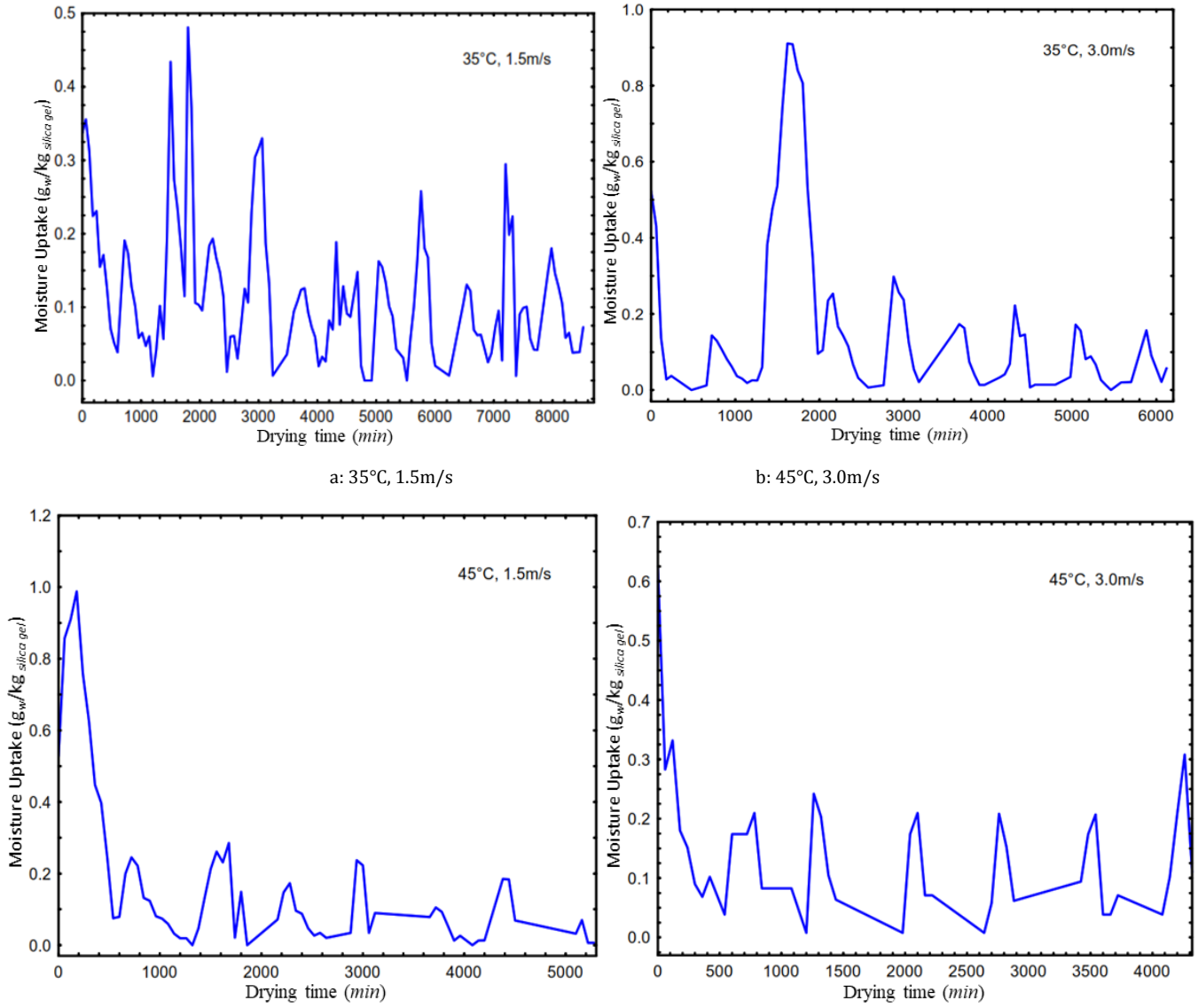

a: 35°C, 1.5m/s b: 45°C, 3.0m/s

Figure 14: Moisture-uptake on silica gel vs. Time

3. Conclusion

In this work, a general thermal-analysis on the key-components of the solar-assisted dehumidification drying system is carried out, where thin-layer drying experiments with Roselle are conducted. The total drying loads are varied from 21 to 89 kWh. Air blowers and water pumps consumed 33% and 5% of the overall energy, respectively. The solar-fraction average-value is found =25%. It is suggested that for future work to add photovoltaic panels (PV) to generate electricity (to reduce conventional-energy consumption); the water-tank capacity must be increasing to match with area of the solar collector; and the silica-gel columns

References

Adeyanju, A.A., 2015. Thermal energy storage techniques. Sci-Afric Journal of Scientific Issues, Research and Essays, 3, (5), Pp. 726-736.

Aijaz, M.A., and Ravikumar, T.S., 2012. Design and Analysis of a Heat Exchanger Network. Material Science Research India, 9 (1), Pp. 85-91, http://dx.doi.org/10.13005/msri/090111

Aissaoui, F., Benmachiche, A.H., Brima, A., Bahloul, D., and Belloufi, Y., 2016. Experimental and Theoretical Analysis on Thermal Performance of the Flat Plate Solar Air Collector. International Journal of Heat and Technology, 34 (2), Pp. 213-220, https://doi.org/10.18280/ijht.340209

Akpinar, E.K., Midilli, A., and Bicer, Y., 2006. The first and second law analyses of thermodynamic of pumpkin drying process. Journal of Food Engineering, 72 (4), Pp. 320-331, https://doi.org/10.1016/j.jfoodeng.2004.12.011

Azharul, K.M., and Hawlader, M.N.A., 2006. Performance evaluation of a v-groove solar air collector for drying applications. Applied Thermal Engineering, 26 (1), Pp. 121-130. https://doi.org/10.1016/j.applthermaleng.2005.03.017

Bardineh, Y.H., Mohamadian, F., Ahmadi, M.H., and Akbarianrad, N., 2018. Medical and dental applications of renewable energy systems. International Journal of Low-Carbon Technologies, 13 (4), Pp. 320-326. https://doi.org/10.1093/ijlct/cty040

Barhoumi, E.M., Okonkwo, P.C., Zghaibeh, M., Belgacem, I.B., Alkanhal, T.A., Abo-Khalil, A.G., and Tlili, I., 2020. Renewable energy resources and workforce case study Saudi Arabia: Review and recommendations. Journal of Thermal Analysis and Calorimetry, 141, Pp. 221-230. https://doi.org/10.1007/s10973-019-09189-2

Beemkumar, N., Karthikeyan, A., Reddy, K.S.K., Rajesh, K., and Anderson, A., 2017. Analysis of Thermal Energy Storage Tank by ANSYS and Comparison with Experimental Results to Improve its Thermal Efficiency. Frontiers in Automobile and Mech. Eng., IOP Conf. Series: Materials Sci. & Eng., 197, Pp. 012039, https://doi.org/10.1088/1757-899X/197/1/012039

Brundrett, G.W., 1987. Handbook of Dehumidification Technology. Butterworths: London, https://www.sciencedirect.com/book/9780408025201/

Buzas, J., Farkas, I., Biro, A. and Nemeth, R. 1998. Modelling and simulation of a solar thermal system. Mathematics and Computers in Simulation, 48, Pp. 33-46, https://doi.org/10.1016/S1474-6670(17)44423-5

Carmona, M., Palacio, M., and Martínez, A., 2017. Experimental analysis of a flat plate solar collector with integrated latent heat thermal storage. Contemporary Urban Affairs, 1 (3), Pp. 7-12, https://doi.org/10.25034/ijcua.2018.3672

Chahartaghi, M., Kalami, M., Ahmadi, M.H., Kumar, R., and Jilte, R., 2019. Energy and exergy analyses and thermoeconomic optimization of geothermal heat pump for domestic water heating. International Journal of Low-Carbon Technologies, 14, Pp. 108-121, https://doi.org/10.1093/ijlct/cty060

Chang, K., Wang, H., and Chung, T., 2004. Effect of regeneration conditions on the adsorption dehumidification process in packed silica gel beds. Applied Thermal Engineering, 24, Pp. 735-742. https://doi.org/10.1016/j.applthermaleng.2003.11.003

Chavan, S., Rudrapati, R., and Manickam, S., 2022. A comprehensive review on current advances of thermal energy storage and its applications. Alexandria Engineering Journal, 61, Pp. 5455-5463, https://doi.org/10.1016/j.aej.2021.11.003

Chen, L.Y., Adi, V.S.K., and Laxmidewi, R., 2022. Shell and tube heat exchanger flexible design strategy for process operability. Case Studies in Thermal Engineering, 37, Pp. 102163, https://doi.org/10.1016/j.csite.2022.102163

Chua, K.J., and Chou, S.K., 2003. Low-cost drying methods for developing countries. Trends in Food Science & Technology, 14 (12), Pp. 519-528. https://doi.org/10.1016/j.tifs.2003.07.003

Condori, M., Echazu, R., and Saravia, L., 2001. Solar drying of sweet pepper and garlic using the tunnel greenhouse drier. Renewable Energy, 22, Pp. 447-460. https://doi.org/10.1016/S0960-1481(00)00098-7

Cüneyt, E., 2017. Basic Design Methods of Heat Exchanger; Chapter 2, in: Heat Exchangers - Design, Experiment and Simulation. Murshed and Lopes (Eds), InTech.: USA, Pp. 10-35, http://dx.doi.org/10.5772/67888

Duffie, J.A., Beckman, W.A., and Blair, N., 2020. Solar Engineering of Thermal Processes, Photovoltaics and Wind 5th ed. John Wiley and Sons, Inc.: Hoboken, NJ., https://doi.org/10.1002/9781119540328

Ebhota, W.S., and Tabakov, P.Y., 2018. The place of small hydropower electrification scheme in socioeconomic stimulation of Nigeria. International Journal of Low-Carbon Technologies, 13 (4), Pp. 311-319, https://doi.org/10.1093/ijlct/cty038

Fernandes, E.J., and Krishanmurthy, S.H., 2022. Design and analysis of shell and tube heat exchanger. Int. J. Simul. Multidisci. Des. Optim, 13 (15), https://doi.org/10.1051/smdo/2022005

Hassan, A., Nikbakht, A.M., Fawzia, S., Yarlagadda, P.K.D.V., and Azharul, K., 2023. Assessment of thermal and environmental benchmarking of a solar dryer as a pilot zero-emission drying technology. Case Studies in Thermal Engineering, 48, Pp. 103084. https://doi.org/10.1016/j.csite.2023.103084

Hassan, Q., 2021. Evaluation and optimization of off-grid and on-grid photovoltaic power system for typical household electrification, Renew Energy, 164, Pp. 375-390. https://doi.org/10.1016/j.renene.2020.09.008

Hou, H.J., Wang, Z.F., Wanga, R.Z., and Wang, P.M., 2005. A new method for the measurement of solar collector time constant. Renewable Energy, 30, Pp. 855-865, https://doi.org/10.1016/j.renene.2004.08.005

Ismael, B.R., and Kumari, A., 2014. Design and Analysis of Heat Exchanger. International Journal of Scientific Engineering and Technology Research, 3 (20), Pp. 4181-4187. Corpus ID: 114001047

Kadam, D.M., and Samuel, D.V.K., 2006. Convective Flat-plate Solar Heat Collector for Cauliflower Drying. Biosystems Engineering, 93 (2), Pp. 189-198, https://doi.org/10.1016/j.biosystemseng.2005.11.012

Kakac, S., and Liu, H. 2002. Heat exchangers: selection, rating, and thermal design. CRC Press: New York.

Kant, K., Shukla, A., Sharma, A., Kumar, A., and Jain, A., 2016. Thermal energy storage based solar drying systems: A review. Innovative Food Science and Emerging Technologies, 34, Pp. 86-99. http://dx.doi.org/10.1016/j.ifset.2016.01.007

Karsli, S., 2007. Performance analysis of new-design solar air collectors for drying applications. Renewable Energy, 32, Pp. 1645-1660, https://doi.org/10.1016/j.renene.2006.08.005

Khayal, O.M.E.S., 2018. Fundamentals of heat exchangers. International Journal of Research in Computer Applications and Robotics, 6 (12), Pp. 1-11.

Kumar, K., and Singh, S., 2022. Investigating Thermal Stratification in a Hot Water Storage Tank during Charging Mode. International Symposium on Fluids and Thermal Engineering (FLUTE 2021). Journal of Physics: Conference Series 2178, Pp. 012001, https://doi.org/10.1088/1742-6596/2178/1/012001

Kushwah, A., Pandey, K.D., Gupta, A., and Saxena, G., 2017. Thermal Modeling of Heat Exchanger: A Review. International Journal of Advance Research in Engineering, Science and Technology, 4 (1), Pp. 30-35.

Lienhard, I.V., and Lienhard, V.J.H., 2008. A Heat Transfer Textbook, 3rd Ed. Cambridge: Phlogiston Press.

Luan, N.T., and Phu, N.M., 2020. Thermohydraulic correlations and exergy analysis of a solar air heater duct with inclined baffles. Case Studies in Thermal Engineering, 21, Pp. 100672. https://doi.org/10.1016/j.csite.2020.100672

Manglam, M.K., Maheshwar, S., Sinha, R.K., and Giri, A., 2023. Thermal modelling and economic analysis of solar collector assisted desalination system with humidification-dehumidification. Tuijin Jishu/Journal of Propulsion Technology, 44 (6), Pp. 3807-3815.

Mondal, D., Rabbi, M.F., and Moral, M.N.A., 2014. Design construction and performance test of a cross flow heat exchanger. Proceedings of the 15th Annual Paper Meet, 07-08 Feb. 2014, Dhaka, Bangladesh

Mujumdar, A.S., 1995. Handbook of industrial drying. Marcell Dekker: New York, https://doi.org/10.1201/9781420017618

Nazari, M., Jafarmadar, S., and Khalilarya, S., 2022. Exergy and thermoeconomic analyses of serpentine tube flat-plate solar water heaters coated with CuO nanostructures. Case Studies in Thermal Engineering, 35, Pp. 102072, https://doi.org/10.1016/j.csite.2022.102072

Nilay, A., Gupta, V., and Bagri, S., 2017. Performance Analysis of Helical Coil Heat Exchanger Using Numerical Technique. IJSRSET 173442, 3 (5), Pp. 152-156. Corpus ID: 217483632

Orozaliev, J., Botpaev, R., Budig, C., Vajen, K., Frank, E., and Obozov, A.D., 2008. Detailed Air-to-Water Heat Exchanger Model for a Multicomponent Solar Thermal System. Proc. EuroSun, Lisbon (PT), 7. - 10.10.2008

Pangavhane, D.R., Sawhney, R.L., and Sarsavadia, P.N., 2002. Design, development and performance testing of a new natural convection solar dryer. Energy, 27 (6), Pp. 579-590. https://doi.org/10.1016/S0360-5442(02)00005-1

Pham, N.D., Khan, M.I.H., and Karim, M.A., 2020. A mathematical model for predicting the transport process and quality changes during intermittent microwave convective drying. Food chemistry, 325, Pp. 126932, https://doi.org/10.1016/j.foodchem.2020.126932

Qusay, H., Abdulrahman, I.S., Salman, H.M., Olapade, O.T., and Jaszczur, M., 2023. Techno-Economic Assessment of Green Hydrogen Production by an Off-Grid Photovoltaic Energy System. Energies, 16 (2), Pp. 744, https://doi.org/10.3390/en16020744

Rabbani, R., and Tariq, I., 2019. Design and analysis of a solar water heating system with thermal storage for residential applications. Journal of Sustainable Energy, 10 (2), Pp. 93-100. https://research.library.mun.ca/14632/1/v10-n2-5.pdf

Rahul, K., Mendiburu, A.Z., Verma, S.K., Gupta, N.K., Sharma, A., Alam, T., and Eldin, S.M., 2023. Experimental assessment and modeling of solar

air heater with V shape roughness on absorber plate. Case Studies in Thermal Engineering, 43, Pp. 102784, https://doi.org/10.1016/j.csite.2 023.102784

Raju, K.A.K.M., Reddy, M.V.K., and Nagaraja, A., 2014. Design Optimization of Cross Flow Heat Exchanger. International Journal of Engineering Research and Technology (IJERT), 3 (2), https://doi.org/10. 17577/IJERTV3IS20091

Rasha, R., 2020. Solar water heating systems with thermal storage for application in newfoundland. Master of Engineering thesis, Faculty of Engineering and Applied Science, Memorial University of Newfoundland, https://research.library.mun.ca/14362/1/thesis.pdf

Reddy, V.K., Mastanaiah, M., and Reddy, R.K., 2015. Experimental analysis of partial and fully charged thermal stratified hot water storage tanks. International Journal of Mechanical Engineering and Technology (IJMET), 6 (2), Pp. 62-69, Corpus ID: 73644867

Sacilik, K., 2007. Effect of drying methods on thin-layer drying characteristics of hull-less seed pumpkin (Cucurbita pepo L.). Journal of Food Engineering, 79, Pp. 23-30. https://doi.org/10.1016/j.jfoo deng.2006.01.023

Sameti, M., Kasaeian, A., Mohammadi, S.S., and Sharifi, N., 2014. Thermal performance analysis of a fully mixed solar storage tank in a ZEB hot water system. Sustainable Energy, 2 (2), Pp. 52-56. https://doi.org/10 .12691/rse-2-2-3

Sarbu, I., and Sebarchievici, C., 2018. A Comprehensive Review of Thermal Energy Storage. Sustainability. 10: 191, https://doi:10.3390/su10010 191

Sari, F.D., Ambarita, H., Napitupulu, F.H., and Kawai, H., 2015. Study on effectiveness of continuous solar dryer integrated with desiccant thermal storage for drying cocoa beans Case Studies in Thermal Engineering, 5, Pp. 32-40. http://dx.doi.org/10.1016/j.csite. 2014.11.003

Stehli, D., and Escher, F., 1990. Design and continuous operation of a solar convection drier with an auxiliary heating system. Drying technology, 8 (2), Pp. 241-260, https://doi.org/10.1080/07373939008959882

Sukhatme, S.P., 2002. Solar energy principles of thermal collector and storage, 2nd Ed. Tata McGraw-Hill Publishing Co.: New Delhi.

Tao, W., Yang, T., Chang, Y., Li-Kai, L., Chang, and Chung, T., 2004. Effects of Moisture on the Adsorption of Volatile Organic Compounds by Zeolite 13X. Journal of environmental engineering, 130, (10), Pp. 1210-1216. https://doi.org/10.1061/(ASCE)0733-9372(2004)130:10(1210)

Wang, Y., M., Li, Qiu, Y., Yu, Q., Luo, X., Li, G., and Ma, X., 2019. Performance analysis of a secondary heat recovery solar-assisted heat pump drying system for mango. Energy Exploration & Exploitation, 37 (4), Pp. 1377-1387. https://doi.org/10.1177/0144598718823937

Yasunaga, T., Noguchi, T., Morisaki, T., and Ikegami, Y., 2018. Basic Heat Exchanger Performance Evaluation Method on OTEC J. Mar. Sci. Eng., 6 (2), Pp. 32. https://doi.org/10.3390/jmse6020032

Zhang, Z., Zhang, H., Yuan, H., Zheng, X., and Mei, N., 2023. Design and experimental analysis of energy-saving and heat storage of a hot water tank based on the source-sink matching principle. Case Studies in Thermal Engineering, 41, Pp. 1-10. 102672, https://doi.org/10.101 6/j.csite.2022.102672

Zhao, J., Reda, S.A., Al-Zahrani, K.S., Singh, P.K., Amin, M.T., Tag-Eldin, E., and Emami, F., 2022. Hydro-thermal and economic analyses of the air/water two-phase flow in a double tube heat exchanger equipped with wavy strip turbulator. Case Studies in Thermal Engineering, 37, Pp. 102260. https://doi.org/10.1016/j.csite.2022.102260

Zohuri, B., 2017. Compact Heat Exchangers Selection, Application, Design and Evaluation. Springer: Switzerland, https://doi.org/10.1007/978-3-319-29835-1